

# Past foraminiferal acclimatization capacity is limited during future warming

<https://doi.org/10.1038/s41586-024-08029-0>


Rui Ying<sup>1</sup>✉, Fanny M. Monteiro<sup>2</sup>, Jamie D. Wilson<sup>3</sup>, Malin Ödalen<sup>4,5</sup> & Daniela N. Schmidt<sup>1</sup>

Received: 31 August 2023

Accepted: 6 September 2024

Published online: 13 November 2024

Open access

 Check for updates

Climate change affects marine organisms, causing migrations, biomass reduction and extinctions<sup>1,2</sup>. However, the abilities of marine species to adapt to these changes remain poorly constrained on both geological and anthropogenic timescales. Here we combine the fossil record and a global trait-based plankton model to study optimal temperatures of marine calcifying zooplankton (foraminifera, Rhizaria) through time. The results show that spinose foraminifera with algal symbionts acclimatized to deglacial warming at the end of the Last Glacial Maximum (LGM, 19–21 thousand years ago, ka), whereas foraminifera without symbionts (non-spinose or spinose) kept the same thermal preference and migrated polewards. However, when forcing the trait-based plankton model with rapid transient warming over the coming century (1.5 °C, 2 °C, 3 °C and 4 °C relative to pre-industrial baseline), the model suggests that the acclimatization capacities of all ecogroups are limited and insufficient to track warming rates. Therefore, foraminifera are projected to migrate polewards and reduce their global carbon biomass by 5.7–15.1% (depending on the warming) by 2100 relative to 1900–1950. Our study highlights the different challenges posed by anthropogenic and geological warming for marine plankton and their ecosystem functions.

Climate change affects marine biodiversity and ecosystem function<sup>1</sup>. In response to warming, some marine organisms, such as fish, have shifted their habitat to track suitable temperatures<sup>2–4</sup>. In addition, some species have maintained or even increased performance in their local habitat through evolutionary adaptation or non-evolutionary acclimatization, both of which are commonly observed in marine microorganisms (plankton)<sup>5–7</sup>. However, the adaptive capacity of plankton and its limits remain poorly constrained in response to both past environmental changes and the ongoing climate crisis. This lack of knowledge causes uncertainty in estimating extinction risk<sup>8</sup>, distribution shifts<sup>2,9</sup> and effects on the marine food web<sup>10</sup> in response to a future warmer climate.

Planktic foraminifera are calcifying zooplankton and contribute roughly half of the modern global pelagic calcium carbonate production<sup>11</sup>. Their comprehensive microfossil records have been used to estimate the realized niche (the observed living conditions) of foraminifera through the late Quaternary glacial–interglacial climatic cycles<sup>12,13</sup>. Specifically, foraminifera were thought to have a limited potential to adaptively change ecological niches across time<sup>12,13</sup>. However, studies revealed that some foraminifera species could exhibit great plasticity in their optimal niche (the subset of the realized niche with the highest fitness)<sup>13</sup>, and extensive morphological, physiological and developmental plasticity that facilitates responses to modern<sup>14</sup> and past<sup>15</sup> environmental changes. This apparent disagreement between niche stability and plasticity leaves a key question open about the adaptive potential and vulnerability of the planktic ecosystem.

Here we aim to understand the adaptive capacity of foraminifera in response to environmental change at different rates and amplitudes

by drawing on the extensive foraminiferal microfossil record and a novel trait-based model. We apply an Earth system model of intermediate complexity (cGENIE) to (a) the LGM (19–21 ka, around 6 °C cooler than the pre-industrial era); (b) the pre-industrial era (1765–1850); and (c) the next century (2100) under 1.5–4 °C warming scenarios relative to the pre-industrial baseline. The cGENIE Earth system model includes a trait-based mechanistic plankton model<sup>16</sup> that recently incorporated the main foraminifera ecogroups, which are distinguished by the presence or absence of photosynthetic symbionts and the presence or absence of calcareous spines associated with grazing enhancement<sup>17</sup>. Any plankton in the model are allowed to grow anywhere, but the emerging biogeography is constrained by the local abiotic (temperature, nutrient and irradiance) and biotic factors (prey concentration, resource competition and grazing pressure) (Methods). This modelling principle mimics the process of natural selection and supports the plasticity of the plankton niche instead of specifying niche parameters<sup>18</sup>.

The mechanistically simulated foraminiferal thermal performance curves (TPCs: abundance as a function of temperature) represent realized niches and are compared with estimates based on fossil abundance in well-dated marine sediments and temperature reconstructions for the LGM and pre-industrial era (Methods). On the basis of the TPCs, the optimal temperatures are quantified as the temperature range that leads to abundances exceeding half of the highest abundance, as shown in a previous report<sup>19</sup>. We regard a shift in optimal temperatures with warming as the signature of adaptive behaviour exemplified by higher growth rates or abundance as defined in previous experimental studies (Extended Data Fig. 1). However, because of the lack of absolute

<sup>1</sup>School of Earth Sciences, University of Bristol, Bristol, UK. <sup>2</sup>School of Geographical Sciences, University of Bristol, Bristol, UK. <sup>3</sup>Department of Earth, Ocean and Ecological Sciences, University of Liverpool, Liverpool, UK. <sup>4</sup>GEOMAR Helmholtz Centre for Ocean Research Kiel, Kiel, Germany. <sup>5</sup>Department of Meteorology, Stockholm University, Stockholm, Sweden. ✉e-mail: rui.ying@bristol.ac.uk

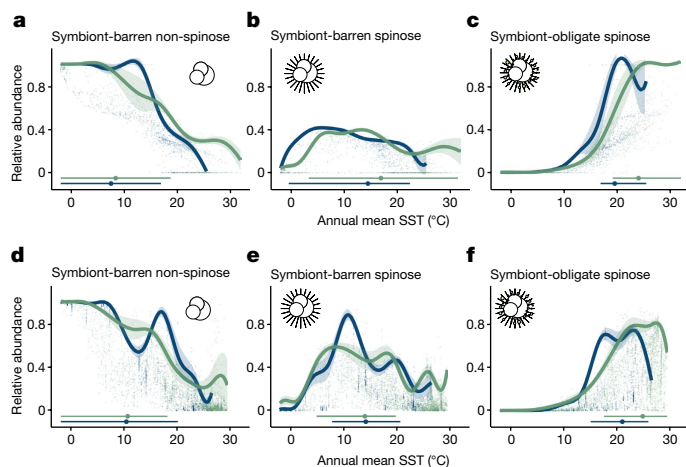


**Fig. 1 | Reconstructed thermal performance of planktic foraminiferal ecogroups.** The thermal performance of planktic foraminiferal ecogroups is reconstructed for the LGM (blue; 19–21 ka) and for the pre-industrial climate (green; 0 ka). **a–f**, Relative abundance of foraminifera ecogroups in the cGENIE model (**a–c**) and the fossil record (**d–f**), along with annual mean sea surface temperature (SST). Both model and observation show a stable thermal niche for symbiont-barren non-spinose foraminifera (**a,d**) and a shifted niche for symbiont-obligate spinose foraminifera (**c,f**) from the LGM to the pre-industrial age. The model–data mismatch (**b,e**) occurs for symbiont-barren spinose foraminifera probably because of the local adaptation of *G. bulloides* in this group<sup>22</sup>. All of the thermal performance curves or thermal niche envelopes (continuous lines) are estimated using an ensemble quantile regression model from 90th–99th levels and calculating the mean and s.d. (in the shading area). The raw data are plotted as shaded dots. The fossil sample size is for 1,433 for the LGM and 4,205 for the pre-industrial age. Optimal temperatures that exceed the 50% maximum abundance in both ages are labelled using horizontal bars (minimum to maximum), with the mean value shown as a dot. The foraminifera icon is for illustration and does not indicate a specific species.

flux (accumulation rate) data in micropalaeontology studies, we use relative abundance here to determine the optimal condition of each species and the adaptive capacity of the whole assemblage. Such relative representations of foraminiferal optimal condition are consistent with experimental measurements<sup>20</sup> and estimates based on maximal body size<sup>21</sup> (Extended Data Table 1), confirming that they can act as a proxy of optimal condition.

### Foraminiferal niche in the LGM and pre-industrial era

In response to the environmental change from the LGM to the pre-industrial era, both the model and the data for foraminifera ecogroups show diverse responses. The symbiont-barren (that is, no symbiont) non-spinose foraminifera retained their optimal temperature at 8/10 °C (model/observation) during the deglacial transition (Fig. 1a,d). This niche stability caused a contraction of geographical range into the high latitudes from the glacial to the pre-industrial (Extended Data Fig. 2). The symbiont-barren spinose foraminifera are an opportunistic (high-food) group dominated by the species *Globigerina bulloides*. The model suggests a wider optimal habitat than the data, with a mean value shifting from 15 °C to 17 °C in comparison with the retained 14 °C in the data (Fig. 1b,e). The model–data mismatch highlights the difficulty of identifying the optimal conditions for cryptic species with multiple genotypes in *G. bulloides* and their specific thermal sensitivities<sup>22</sup> with one ecological setting in the model. Specifically, the model cannot differentiate between the open ocean types found in temperate waters and the upwelling types associated with the coastal high-nutrient settings. Finally, for symbiont-obligate spinose foraminifera that occupy the shallow and warm open oceans in the mid-to-low latitudes, the

modelled and observed optimal temperature both increased from 20/21 °C (LGM model/observation) to 24/25 °C (pre-industrial model/observation) (Fig. 1c,f and Extended Data Fig. 2).

The fossil data allow us to further investigate species-level responses. We reconstructed the TPCs of 31 foraminifera species on the basis of LGM and pre-industrial fossil observations, extending our analysis to species that do not belong to the above ecogroups (Extended Data Fig. 3 and Extended Data Table 1). Our species-based results agree with and expand previous findings about species-dependent thermal niches<sup>13</sup>. Although some species exhibited niche stability (*G. bulloides* and *Neogloboquadrina pachyderma*), others shifted their optimal niche towards colder (*Orbulina universa*, *Neogloboquadrina incompta* and *Turborotalita quinqueloba*) or warmer (*Globigerinoides ruber albus*, *Globigerinoides ruber ruber*, *Trilobatus sacculifer*, *Neogloboquadrina dutertrei* and *Pulleniatina obliquiloculata*) environments. However, in this species-level analysis, changes in thermal optima cannot be explained by ecological traits such as symbiosis or spines (two-way ANOVA, symbiosis:  $F_{4,26} = 1.248, P = 0.321$ ; spine:  $F_{1,26} = 0.228, P = 0.638$ ). The discrepancy between species- and ecogroup-level analysis suggests that our ecogroup-level model captures the response of dominant foraminifera but ignores the interspecies ecological differences of rare taxa.

The shift in the TPC of symbiotic foraminifera provides evidence of their adaptive abilities to warming. Although the TPCs are based on relative abundance data, our results cannot be explained by species replacement alone, because modelled (Extended Data Fig. 4) and observed absolute abundance (foraminifera accumulation rates) have increased since the LGM<sup>23</sup>, reflecting their unambiguously increased fitness under warming. Similarly, these results are not caused by dispersal limitation or by a lack of warm habitats in the LGM, because these processes modify the boundary rather than the shape of the TPC (Extended Data Fig. 1). Finally, we have reanalysed niche reconstruction data from a previous study<sup>12</sup>, which shows a similarly increasing optimal temperature from the LGM to the pre-industrial era (−0.3 °C to 8.6 °C) (Extended Data Fig. 5 and Supplementary Methods). This confirms the robustness of our results, because the same response is detected independent of evidence used: relative abundance, presence–absence, accumulation rate or model simulation.

We interpret the adaptive response of symbiont-obligate foraminifera shown in the data and our model during the deglacial warming as acclimatization, which we define as the non-evolutionary reversible response of a species to maintain or increase performance<sup>5,24,25</sup>. This interpretation of acclimatization is based on the knowledge that no novel species or trait emerged across the planktonic foraminifera taxa since the LGM (that is, no evolutionary adaptation). Previous studies<sup>26,27</sup> show that the most recent origination amongst modern morphologically defined foraminifera species occurred diachronously from 2.2–32.2 million years ago, hence much earlier than the LGM (19–21 ka). Although there is evidence for genetic changes within the foraminiferal morphotypes (termed as ‘cryptic species’), the most recent genetic split occurred during marine isotope stage 5.5 (roughly 120 ka)<sup>28</sup>—again, earlier than the LGM. Moreover, the symbiont-obligate foraminifera ecogroup, which presents the optimal niche change during the deglaciation, has the least cryptic species in the community<sup>29</sup>. Furthermore, the dominant species (*T. sacculifer*) in this ecogroup has no cryptic species. This reinforces that no genetic divergence occurred since the LGM to support a possible interpretation of evolutionary change of foraminifera species.

### Projection of foraminifera by 2100

Given the thermal response identified in the past, it is possible to consider whether acclimatization to future warming will allow foraminifera to maintain their biomass and ecosystem functions. To answer this question, we conducted a series of transient simulations from a pre-industrial climate to 2100 using the same model used for the last

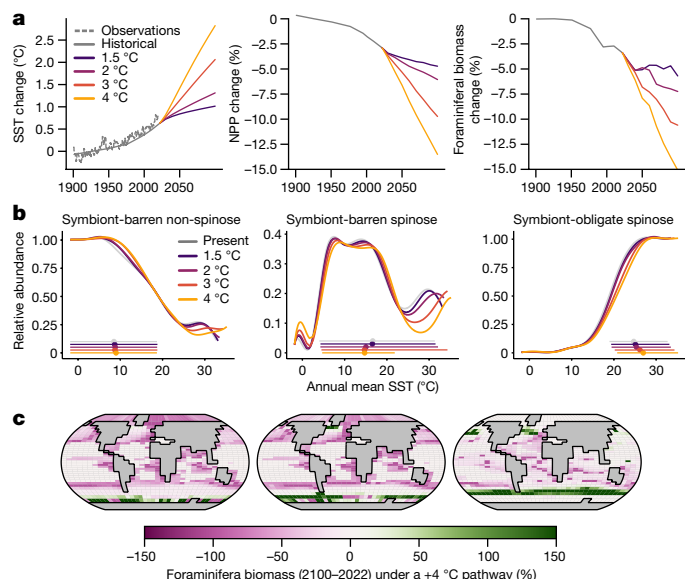


**Fig. 2 | Response of plankton ecosystems to future warming in cGENIE.** **a**, Modelled change in SST, NPP and globally integrated foraminifera carbon biomass when global mean surface temperature increases by 1.5 °C, 2 °C, 3 °C and 4 °C in 2100 relative to the 1900–1950 average. We used historical CO<sub>2</sub> to force the model (with comparison with ERSST v.5 (ref. 48) SST observations), and linear CO<sub>2</sub> forcings to mimic future warming. **b**, Thermal performance curves of the three foraminifera ecogroups in 2100 as estimated in Fig. 1. The grey curves show the present niches. **c**, Carbon biomass future trend for each foraminifera group in response to a 4 °C warming by 2100 relative to the present. All biomass in this figure refers to biomass standing stock, but the trend is the same for biomass production rate (Supplementary Fig. 7).

deglacial warming experiment. We used historical CO<sub>2</sub> concentrations to force the model from pre-industrial to the present day (2022), and four idealized linear CO<sub>2</sub> forcings to simulate future warming scenarios (1.5 °C, 2 °C, 3 °C and 4 °C by 2100 relative to the 1900–1950 average; Fig. 2a and Supplementary Fig. 2). By reproducing the observation that the global mean sea surface temperature (SST) in the present day (2022) is around 0.6 °C warmer than the 1900–1950 average (Fig. 2a), the model demonstrates its ability to simulate future scenarios in terms of the rate of warming. By 2100, the global SST will increase by 1.0 °C, 1.3 °C, 2.1 °C and 2.8 °C in response to the different warming forcings. The resulting ocean net primary productivity (NPP) drops by 4.7%, 6.1%, 9.7% and 13.5%, respectively (Fig. 2a), in good agreement with the Coupled Model Intercomparison Project (CMIP5–CMIP6) range (Supplementary Fig. 3).

The modelled foraminifera show limited thermal adaptive potentials in the future (Fig. 2b). The mean thermal optima of symbiont-barren non-spinose foraminifera only shift by 0.0 °C, 0.2 °C, 0.2 °C and 0.5 °C compared to the present day (2022) under our four warming scenarios. The mean optimal temperature for symbiont-barren spinose foraminifera decreases by 1.7 °C, 1.5 °C, 1.2 °C and 0.6 °C as their tropical habitats vanish by 2100. Symbiont-obligate foraminifera are projected to have a greater acclimatization, with 0.4 °C, 0.7 °C, 1.5 °C and 2.3 °C shifts in optima temperature, comparable with the response to deglacial warming (Fig. 1). However, the reduction in the absolute abundance of symbiont-obligate foraminifera indicates that optimal temperature changes are more limited than it seems (0.4 °C, 0.7 °C, 1.2 °C and 1.8 °C on the basis of absolute abundance). Our simulations indicate that, even when the possibility of acclimatization is accounted for in the model, planktonic foraminifera will not be able to track the pace of future warming.

As observed since the pre-industrial age<sup>30,31</sup>, planktic foraminifera in the mid-to-high latitudes will migrate polewards in the future.

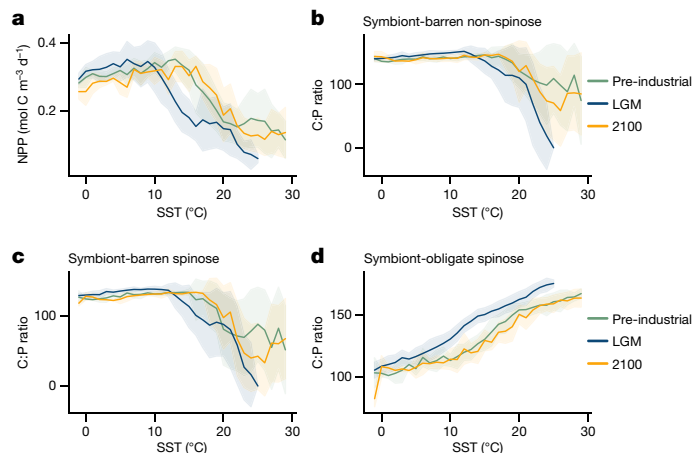


**Fig. 3 | Ecological and physiological drivers of change in foraminiferal thermal performance.** **a**, NPP (line, mean; shaded area, s.d.) for each temperature bin (1 °C). **b–d**, The cellular C:P biomass ratio of foraminifera ecogroups (symbiont-barren non-spinose (**b**), symbiont-barren spinose (**c**) and symbiont-obligate spinose (**d**)) determines the assimilation efficiency of prey. A clear change in the NPP–temperature relationship occurred from the LGM to the pre-industrial era but is not seen in the future under a 4 °C warming scenario, explaining the different responses between the two warming events. The distinct C:P shift indicates the physiological adjustment of symbiont-obligate spinose foraminifera under different trophic conditions.

Symbiont-barren spinose foraminifera, such as *G. bulloides*, will increase their biomass standing stocks (hereafter, biomass) in the Southern Ocean and the North Atlantic, benefitting from niche expansion (Fig. 2c) into a habitat in which symbiont-barren non-spinose species dominate today<sup>32</sup>. The biomass of warm-adapted symbiont-obligate spinose will increase in the North subpolar regions and subantarctic zones (Fig. 2c), which agrees with the observations in the Arctic<sup>33</sup> and Southern Ocean<sup>34</sup>.

Overall, the global biomass of foraminifera is predicted to decline in the future (Fig. 2a,c and Extended Data Fig. 6). The model estimates that global foraminifera biomass has already decreased by 3.4% at present (2022) relative to the 1900–1950 average (Fig. 3a). With a warming of 1.5, 2, 3, and 4 °C by 2100, foraminifera biomass is projected to reduce further by 5.7, 7.2, 10.6 and 15.1%, respectively (Fig. 2a). This biomass loss is widespread across the ocean, except in the Southern Ocean and to a lower extent in the North subpolar regions, where species replacement occurs (Fig. 2c). The loss of biomass is uneven across ecogroups and is driven mainly by the two symbiont-barren groups (9–23% and 10–27% for non-spinose and spinose, respectively), which account for around 77% of the total change (Extended Data Fig. 6). We suggest that this preferential loss is caused by the reliance of these groups on phytoplankton as prey, which are also decreasing in biomass (Fig. 2a). By contrast, symbiotic foraminifera show lower losses (4–10% biomass loss; Extended Data Fig. 6), because they can draw on multiple energy pathways, highlighting the importance of ecological redundancy to reduce overall losses in biomass. Our model results are well supported by census counts of planktic foraminifers spanning the past century<sup>31</sup>. It should be noted that our model does not include the risk of symbiont bleaching; this has been suggested to affect foraminiferal physiology in past warm events<sup>35</sup>, is evident today in coral symbionts<sup>36</sup> and would increase the vulnerability of the group.

### Role of food in acclimatization

The foraminiferal response in the past and future allows us to examine the mechanism of acclimatization. To understand the details, we disentangled the ecophysiological processes that account for the plankton

performance. The modelled plankton growth rate monotonically increases with temperature and is modulated by nutrient availability<sup>37</sup>. The top-down control (grazing pressure) is typically negligible for foraminifera, owing to their small biomass<sup>38</sup>. The modelled biomass loss, including the mortality and respiration rate, has the same thermal sensitivity across different climates and seems not to contribute to the observed change in thermal niche (Supplementary Methods). Therefore, the modelled thermal acclimatization is likely to be driven by changes in prey availability (grazing source) and prey quality (assimilation efficiency), and by autotrophic input from symbionts that support the metabolic needs for living at higher temperatures.

We investigate the role of food by comparing the ocean's primary production and temperature for the LGM, pre-industrial era and future in response to the +4 °C scenario. The NPP–SST relationship is similar across the time slices at high latitudes (lower than 10 °C), but different at low latitudes (higher than 10 °C) (Fig. 3a). This difference explains the stable niche of the symbiont-barren non-spinose ecogroup, which is heterotrophic and tracks the footprint of the primary producers (Figs. 1 and 3a–c). For a more detailed understanding, we analysed the foraminiferal cellular physiology (variable stoichiometry)<sup>39</sup> to determine the prey assimilation efficiency. We found a nearly linear increase in the carbon to phosphate (C:P) biomass ratio of symbiont-obligate foraminifera with temperature (Fig. 3d), indicating a more efficient use of nutrients in warm oligotrophic environments. The C:P ratio decreases because more prey (indicated by NPP) can be found in warmer environments during the pre-industrial era, compared with the LGM (Fig. 3a). This supports the hypothesis that symbiont-obligate foraminifera benefit from symbiosis to supplement metabolic needs, whereas symbiont-barren foraminifera depend on food availability, as observed in culture studies in which algal symbionts transfer carbon-enriched polysaccharide (for example, starch) through lipid droplets to the host cytoplasm<sup>40</sup>. This energy transfer allows the host with a high affinity to nutrients to counteract nutrient scarcity. Our interpretation is further supported by the observation that the foraminiferal nutrient content (size-normalized protein) is determined by NPP and chlorophyll *a* concentrations<sup>41</sup>.

The different pattern of NPP–SST for future scenarios compared with the LGM corroborates the distinction between past and ongoing warming (Fig. 3a). The deglacial warming was associated with active ocean mixing and a higher nutrient supply<sup>42,43</sup>, whereas the modern warming is characterized by increasing stratification. The abrupt current warming determines the climatic impacts on the ocean circulation, ice sheets, wind stress and nutrient supply, which are distinctly different from the LGM changes. To validate the importance of this, we forced the model to reach the same warming magnitude but at different rates. All experiments show ocean stratification and reduced nutrient delivery to the surface (Extended Data Fig. 7). However, in response to slower warming scenarios, ocean circulation can mitigate the stratification and allow a greater amount of nutrients to be supplied to the upper layers, especially in the Southern Ocean (Extended Data Figs. 8 and 9).

## Implications

Marine plankton support the flux of energy and material through the marine food web and the storage of carbon in the ocean. Consequently, their adaptive capacity directly influences fishery production and the global carbon cycle. Our study provides several lines of evidence for acclimatization in marine calcifying zooplankton on various geological timescales, and suggests that this acclimatization depends on ecology and food supply. The difference in response to past, present and future warming highlights the unprecedented risks for the marine plankton ecosystem, which could be further exacerbated by ocean acidification<sup>44</sup>, symbiont bleaching<sup>35</sup>, deoxygenation<sup>45</sup> and other potentially synergistic stressors. The importance of the rate of change in determining the capacity of foraminifera acclimatization agrees with a previous

modelling study<sup>46</sup>, which came to similar conclusions about the phytoplankton's adaptive responses. However, to fundamentally understand these risks, assessments of plankton life cycles are needed to work out how changing environments select phenotypes in the offspring population<sup>47</sup> and influence their ontogeny. Overall, the acceleration of present climate change is challenging the adaptive capacity of marine plankton and their ecosystem functioning.

## Online content

Any methods, additional references, Nature Portfolio reporting summaries, source data, extended data, supplementary information, acknowledgements, peer review information; details of author contributions and competing interests; and statements of data and code availability are available at <https://doi.org/10.1038/s41586-024-08029-0>.

- Cooley, S. et al. in *Climate Change 2022: Impacts, Adaptation and Vulnerability. Contribution of Working Group II to the Sixth Assessment Report of the Intergovernmental Panel on Climate Change* (eds Pörtner, H.-O. et al.) 379–550 (Cambridge Univ. Press, 2022).
- Yasuhara, M. et al. Past and future decline of tropical pelagic biodiversity. *Proc. Natl Acad. Sci. USA* **117**, 12891–12896 (2020).
- Pinsky, M. L., Worm, B., Fogarty, M. J., Sarmiento, J. L. & Levin, S. A. Marine taxa track local climate velocities. *Science* **341**, 1239–1242 (2013).
- Chaudhary, C., Richardson, A. J., Schoeman, D. S. & Costello, M. J. Global warming is causing a more pronounced dip in marine species richness around the equator. *Proc. Natl Acad. Sci. USA* **118**, e2015094118 (2021).
- Padfield, D., Yvon-Durocher, G., Buckling, A., Jennings, S. & Yvon-Durocher, G. Rapid evolution of metabolic traits explains thermal adaptation in phytoplankton. *Ecol. Lett.* **19**, 133–142 (2016).
- Irwin, A. J., Finkel, Z. V., Müller-Karger, F. E. & Troccoli Ghinaglia, L. Phytoplankton adapt to changing ocean environments. *Proc. Natl Acad. Sci. USA* **112**, 5762–5766 (2015).
- Lee, Y. H. et al. Epigenetic plasticity enables copepods to cope with ocean acidification. *Nat. Clim. Change* **12**, 918–927 (2022).
- Yasuhara, M., Hunt, G., Dowsett, H. J., Robinson, M. M. & Stoll, D. K. Latitudinal species diversity gradient of marine zooplankton for the last three million years. *Ecol. Lett.* **15**, 1174–1179 (2012).
- Chivers, W. J., Walne, A. W. & Hays, G. C. Mismatch between marine plankton range movements and the velocity of climate change. *Nat. Commun.* **8**, 14434 (2017).
- Lotze, H. K. et al. Global ensemble projections reveal trophic amplification of ocean biomass declines with climate change. *Proc. Natl Acad. Sci. USA* **116**, 12907–12912 (2019).
- Neukermans, G. et al. Quantitative and mechanistic understanding of the open ocean carbonate pump - perspectives for remote sensing and autonomous in situ observation. *Earth Sci. Rev.* **239**, 104359 (2023).
- Antell, G. S., Fenton, I. S., Valdes, P. J. & Saupe, E. E. Thermal niches of planktonic foraminifera are static throughout glacial–interglacial climate change. *Proc. Natl Acad. Sci. USA* **118**, e2017105118 (2021).
- Waterson, A. M., Edgar, K. M., Schmidt, D. N. & Valdes, P. J. Quantifying the stability of planktic foraminiferal physical niches between the Holocene and Last Glacial Maximum: niche stability of planktic foraminifera. *Paleoceanography* **32**, 74–89 (2017).
- Davis, C. V., Wishner, K., Renema, W. & Hull, P. M. Vertical distribution of planktic foraminifera through an oxygen minimum zone: how assemblages and test morphology reflect oxygen concentrations. *Biogeosciences* **18**, 977–992 (2021).
- Vanadzina, K. & Schmidt, D. N. Developmental change during a speciation event: evidence from planktic foraminifera. *Paleobiology* **48**, 120–136 (2022).
- Ward, B. A. et al. EcoGenIE 1.0: plankton ecology in the cGenIE Earth system model. *Geosci. Model Dev.* **11**, 4241–4267 (2018).
- Ying, R., Monteiro, F. M., Wilson, J. D. & Schmidt, D. N. ForaminiferaGenIE 2.0: incorporating symbiosis and spine traits into a trait-based global planktic foraminiferal model. *Geosci. Model Dev.* **16**, 813–832 (2023).
- Follows, M. J., Dutkiewicz, S., Grant, S. & Chisholm, S. W. Emergent biogeography of microbial communities in a model ocean. *Science* **315**, 1843–1846 (2007).
- Sinclair, B. J. et al. Can we predict ectotherm responses to climate change using thermal performance curves and body temperatures? *Ecol. Lett.* **19**, 1372–1385 (2016).
- Lombard, F., Labeyrie, L., Michel, E., Spero, H. J. & Lea, D. W. Modelling the temperature dependent growth rates of planktic foraminifera. *Mar. Micropaleontol.* **70**, 1–7 (2009).
- Schmidt, D. N., Renaud, S., Bollmann, J., Schiebel, R. & Thierstein, H. R. Size distribution of Holocene planktic foraminifera assemblages: biogeography, ecology and adaptation. *Mar. Micropaleontol.* **50**, 319–338 (2004).
- Darling, K. F. et al. Genetic diversity and ecology of the planktonic foraminifera *Globigerina bulloides*, *Turborotalita quinqueloba* and *Neoglobobulimina papyderma* off the Oman margin during the late SW monsoon. *Mar. Micropaleontol.* **137**, 64–77 (2017).
- Steinke, S., Yu, P.-S., Kucera, M. & Chen, M.-T. No-analog planktonic foraminiferal faunas in the glacial southern South China Sea: implications for the magnitude of glacial cooling in the western Pacific warm pool. *Mar. Micropaleontol.* **66**, 71–90 (2008).
- Möller, V. et al. in *Climate Change 2022: Impacts, Adaptation and Vulnerability. Contribution of Working Group II to the Sixth Assessment Report of the Intergovernmental Panel on Climate Change* (eds Pörtner, H.-O. et al.) 2897–2930 (Cambridge Univ. Press, 2022).
- Hattich, G. S. I. et al. Temperature optima of a natural diatom population increases as global warming proceeds. *Nat. Clim. Change* **14**, 518–525 (2024).

26. Sexton, P. F. & Norris, R. D. Dispersal and biogeography of marine plankton: long-distance dispersal of the foraminifer *Truncorotalia truncatulinoides*. *Geology* **36**, 899–902 (2008).
27. Kucera, M. & Schonfeld, J. in *Deep-Time Perspectives on Climate Change: Marrying the Signal from Computer Models and Biological Proxies* (eds Williams, M. et al.) 409–425 (Geological Society of London on behalf of The Micropalaeontological Society, 2007).
28. Vargas, C., de, Renaud, S., Hilbrecht, H. & Pawlowski, J. Pleistocene adaptive radiation in *Globorotalia truncatulinoides*: genetic, morphologic, and environmental evidence. *Paleobiology* **27**, 104–125 (2001).
29. Morard, R. et al. The global genetic diversity of planktonic foraminifera reveals the structure of cryptic speciation in plankton. *Biol. Rev.* **99**, 1218–1241 (2024).
30. Jonkers, L., Hillebrand, H. & Kucera, M. Global change drives modern plankton communities away from the pre-industrial state. *Nature* **570**, 372–375 (2019).
31. Chaabane, S. et al. Modern planktonic Foraminifera: migrating is not enough. Preprint at <https://doi.org/10.21203/rs.3.rs-3485983/v1> (2023).
32. Grigoratou, M., Monteiro, F. M., Wilson, J. D., Ridgwell, A. & Schmidt, D. N. Exploring the impact of climate change on the global distribution of non-spinose planktonic foraminifera using a trait-based ecosystem model. *Glob. Change Biol.* **28**, 1063–1076 (2022).
33. Greco, M., Werner, K., Zamelczyk, K., Rasmussen, T. L. & Kucera, M. Decadal trend of plankton community change and habitat shoaling in the Arctic gateway recorded by planktonic foraminifera. *Glob. Change Biol.* **28**, 1798–1808 (2022).
34. Pinkerton, M. H. et al. Zooplankton in the Southern Ocean from the continuous plankton recorder: distributions and long-term change. *Deep Sea Res. Part I* **162**, 103303 (2020).
35. Edgar, K. M. et al. Symbiont ‘bleaching’ in planktic foraminifera during the Middle Eocene Climatic Optimum. *Geology* **41**, 15–18 (2013).
36. Hughes, T. P. et al. Spatial and temporal patterns of mass bleaching of corals in the Anthropocene. *Science* **359**, 80–83 (2018).
37. Boyd, P. W. Physiology and iron modulate diverse responses of diatoms to a warming Southern Ocean. *Nat. Clim. Change* **9**, 148–152 (2019).
38. Grigoratou, M. et al. A trait-based modelling approach to planktonic foraminifera ecology. *Biogeosciences* **16**, 1469–1492 (2019).
39. Galbraith, E. D. & Martiny, A. C. A simple nutrient-dependence mechanism for predicting the stoichiometry of marine ecosystems. *Proc. Natl Acad. Sci. USA* **112**, 8199–8204 (2015).
40. LeKieffre, C. et al. Assimilation, translocation, and utilization of carbon between photosynthetic symbiotic dinoflagellates and their planktic foraminifera host. *Mar. Biol.* **165**, 104 (2018).
41. Meilland, J., Howa, H., Lo Monaco, C. & Schiebel, R. Individual planktic foraminifer protein-biomass affected by trophic conditions in the Southwest Indian Ocean, 30°S–60°S. *Mar. Micropaleontol.* **124**, 63–74 (2016).
42. Anderson, R. F. et al. Wind-driven upwelling in the Southern Ocean and the deglacial rise in atmospheric CO<sub>2</sub>. *Science* **323**, 1443–1448 (2009).
43. Gray, W. R. et al. Deglacial upwelling, productivity and CO<sub>2</sub> outgassing in the North Pacific Ocean. *Nature Geosci* **11**, 340–344 (2018).
44. Kawahata, H. et al. Perspective on the response of marine calcifiers to global warming and ocean acidification—behavior of corals and foraminifera in a high CO<sub>2</sub> world “hot house”. *Prog. Earth Planet. Sci.* **6**, 5 (2019).
45. Deutsch, C., Penn, J. L. & Seibel, B. Metabolic trait diversity shapes marine biogeography. *Nature* **585**, 557–562 (2020).
46. Sauterey, B. et al. Phytoplankton adaptive resilience to climate change collapses in case of extreme events—a modeling study. *Ecol. Model.* **483**, 110437 (2023).
47. Gunderson, A. R. & Stillman, J. H. Plasticity in thermal tolerance has limited potential to buffer ectotherms from global warming. *Proc. R. Soc. B* **282**, 20150401 (2015).
48. Lan, X., Tans, P. & Thoning, K. W. Trends in globally-averaged CO<sub>2</sub> determined from NOAA Global Monitoring Laboratory measurements. <https://doi.org/10.15138/9N0H-ZH07> (2023).

**Publisher’s note** Springer Nature remains neutral with regard to jurisdictional claims in published maps and institutional affiliations.



**Open Access** This article is licensed under a Creative Commons Attribution 4.0 International License, which permits use, sharing, adaptation, distribution and reproduction in any medium or format, as long as you give appropriate credit to the original author(s) and the source, provide a link to the Creative Commons licence, and indicate if changes were made. The images or other third party material in this article are included in the article’s Creative Commons licence, unless indicated otherwise in a credit line to the material. If material is not included in the article’s Creative Commons licence and your intended use is not permitted by statutory regulation or exceeds the permitted use, you will need to obtain permission directly from the copyright holder. To view a copy of this licence, visit <http://creativecommons.org/licenses/by/4.0/>.

© The Author(s) 2024

## Methods

### cGENIE Earth system model

cGENIE is an Earth system model of intermediate complexity, with a  $36 \times 36$  equal-area grid ( $10^\circ$  longitude and uniform in the sine of latitude) and 16 vertical ocean layers, that resolves multiple biogeochemical cycles. It facilitates the exploration of long-term climate, marine ecology and carbon cycling, particularly in palaeoceanography studies<sup>49</sup>. It couples several components, including a two-dimensional energy–moisture balance (EMBM) atmosphere and a thermodynamic sea-ice model<sup>50</sup>, a three-dimensional ocean circulation (C-GOLDSTEIN)<sup>51</sup> combined with ocean biogeochemistry (BIOGEM)<sup>52</sup> and a trait-based plankton community model (EcoGENIE)<sup>16</sup>. The EcoGENIE model includes a full spectrum of planktic foraminifera ecogroups<sup>17,32</sup> on the basis of the implementation of their functional traits (body size, calcification, symbionts, spines and feeding behaviour). The foraminifera biomass is determined by environmental temperature, prey availability and biotic interaction with other plankton groups. The foraminifera parameterizations have been improved in this study (Supplementary Fig. 5 and Supplementary Table 2). Concrete details can be found in the Supplementary Methods.

**LGM, pre-industrial and future model simulations.** We derive the palaeogeographical configuration, zonal albedo profile and ice-sheet data from the HadCM3 model<sup>53</sup> to configure the cGENIE LGM model. We apply the LGM climate boundary conditions including lower atmospheric  $\text{CO}_2$  (193 ppm), a new dust deposition field<sup>54</sup>, enhanced wind stress<sup>55</sup> and orbital parameters following the PMIP4 protocol<sup>56</sup>. In addition, we apply a brine rejection relocation in the Southern Ocean, which redistributes brine (salt expelled during sea-ice production) from the surface to the deep ocean, following a previous report<sup>57</sup> and based on another study<sup>58</sup>. The parameterizations were constrained by a global compilation of marine carbon stable isotope ( $\delta^{13}\text{C}$ ) data<sup>59</sup>. The simulated LGM ocean shows a weaker and shallower Atlantic Meridional Overturning Circulation (AMOC) than the modern one<sup>57</sup>, agreeing with previous modelling results<sup>60</sup>.

On the basis of these glacial boundary conditions, we spin up the model for 10,000 years to reach a steady state. The model predicts a regionally enhanced carbon export in the LGM compared to the pre-industrial era, as suggested by a multiple-proxy compilation (Supplementary Fig. 1). The LGM SST in cGENIE is around  $5^\circ\text{C}$  cooler than the pre-industrial one, which is overall higher than the data for the LGM, but in agreement with some PMIP4 models<sup>61</sup>. We note that the LGM SST reconstruction uncertainty is still an unsolved question<sup>62</sup>, which can be attributed both to models<sup>61</sup> and proxies<sup>63</sup>.

The pre-industrial experiment adopts a similar grid and carbon-cycle configuration to that described previously<sup>64</sup>. The model is spun up under the pre-industrial state (1765) for 10,000 years, with an atmospheric  $\text{CO}_2$  concentration of 278 ppm and a dust field from a previous report<sup>65</sup>. We next use the historical  $\text{CO}_2$  data as input to force the model to run from the pre-industrial age to the present day (2022)<sup>48</sup>, and impose a series of idealized future  $\text{CO}_2$  forcings causing  $1.5^\circ\text{C}$ ,  $2^\circ\text{C}$ ,  $3^\circ\text{C}$  and  $4^\circ\text{C}$  global air warming, with all the other parameterization the same as for the pre-industrial simulation (Supplementary Fig. 2). For simplicity, we do not include any other greenhouse gases in this study.

The historical global mean surface temperature aligns well with the HadCRUT5 dataset<sup>66</sup>, and the global mean SST agrees with the ERSST v.5 dataset<sup>48</sup> (Supplementary Fig. 2). The future experiment results are comparable with fully coupled CMIP Earth system models. The model predicts the same subtropical and tropical zooplankton biomass loss and polar biomass increment as CMIP6 models<sup>67</sup>. The NPP is projected to decline between 1% ( $1^\circ\text{C}$ ) and 10% ( $4^\circ\text{C}$ ) by 2100 relative to the present day, like the CMIP5 average and the lower bound of CMIP6 (ref. 67) (Supplementary Fig. 3).

**Foraminiferal biomass to abundance.** All of the modelled foraminifera carbon biomass is converted to absolute abundance to determine relative abundance. The conversion follows the equation below, in which biomass and cell volume are taken from the model, and the carbon biomass density uses a foraminifera-average value ( $0.089\text{ pg C } \mu\text{m}^{-3}$ ) derived from refs. 68,69.

$$\text{Abundance} = \text{Biomass} / (\text{Cell volume} \times \text{Density})$$

### LGM and pre-industrial observational data

**LGM and pre-industrial planktic foraminifera abundance data.** We use the curated sediment foraminifera assemblage datasets ForCen<sup>570</sup> and MARGO<sup>71</sup> to represent the pre-industrial and the LGM abundance. The MARGO samples have undergone a quality level assessment based on the age control and have no bias caused by calcite dissolution<sup>71</sup>. Both datasets have global coverage, with a bias towards the low latitudes (Supplementary Fig. 4). We only use relative abundance data and convert absolute count to relative abundance if necessary. We keep the different sample depths in the same sediment core (that is, no averaging) to include the uncertainty within each time interval. After the data standardization (see below), there are 4,205 data points for the pre-industrial age (41 species) and 1,433 data points for the LGM (35 species).

For consistency, we use the latest taxonomic standardization<sup>72</sup> in both datasets. Specifically, we merged *Globorotalia truncatulinoides* sinistral and *G. truncatulinoides* dextral into *G. truncatulinoides*, and *T. sacculifer* with sac and without sac chamber (*Trilobatus trilobus*) into *T. sacculifer*. We separate *G. ruber* into *G. ruber albus* (white) and *G. ruber ruber* (pink) and use *N. pachyderma* and *N. incompta* to replace the *N. pachyderma* sinistral and *N. pachyderma* dextral. The commonly used 'P/D intergrades' is merged into *N. incompta* following the ForCenS dataset<sup>70</sup>. We adopt the use of *Globorotalia cultrata* and *Globorotalia eastropacia* to replace *Globorotalia menardii* and *Globorotalia theyeri*, respectively.

These species-based data are aggregated into functional groups according to their trait of spines and algal symbionts (Supplementary Table 1). The algal symbiont information follows a previous report<sup>73</sup>: 'symbiont-barren' (no symbiont), 'symbiont-obligate' (must live with symbiont), 'symbiont-facultative' (has been found with and without symbionts), 'symbiont-bearing' (newly detected relationship in ref. 73) and 'undetermined'. The spine information is based on a previous report<sup>74</sup> and mikrotax<sup>75</sup> (<https://www.mikrotax.org>), with the classification of 'spinose', 'non-spinose' and 'undetermined'. We report only three groups: 'symbiont-barren non-spinose', 'symbiont-barren spinose' and 'symbiont-obligate spinose', owing to limited biological understanding of the drivers of symbiont-facultative behaviour and its benefits or trade-offs. However, the species-level data are reported as completely as possible for the readers' interest.

**LGM and pre-industrial SST data.** We use the geographical information in the abundance dataset to look up the SST in the nearest grid location within data products. We use the HadISST1 dataset<sup>76</sup> ( $1^\circ \times 1^\circ$ , latitude  $\times$  longitude, 1870–1900 annual mean climatology) as our pre-industrial temperature reference and a previous data assimilation (Tierney et al.<sup>77</sup>) ( $1.9^\circ \times 2.5^\circ$ , latitude  $\times$  longitude) as our LGM reference. Tierney et al.<sup>77</sup> used an Ensemble Kalman filter to incorporate the information of geochemical proxy data compilation (19–23 ka) with the constraints of a climate model (iCESM). The proxy compilation includes organic chemistry-based proxies ( $U_{37}^K$ ,  $\text{TEX}_{86}$ ), and foraminifera-shell-based  $\delta^{18}\text{O}$  and Mg/Ca. Each type of proxy was calibrated using a Bayesian model to propagate proxy uncertainties and seasonal bias. We do not use assemblage-based temperature reconstruction from the MARGO to avoid circular reasoning.

It is worth noting that the temperature data used here only represent the surface layer (0.5 m for LGM data and 0.2 m for HadISST) and its

long-term climatology, therefore not indicating the in situ temperature of the precise habitat. The common and accepted use of annual mean SST averages over the seasonal variability does not reflect the dynamic vertical distribution of foraminifera. These limitations do not affect our inference of acclimatization because a shallow thermocline in the high latitudes restricts most species to the surface layer, whereas the symbiont-bearing species in the low latitudes need to live in the mixed layer to obtain sufficient solar irradiance<sup>78</sup>. This gives us faith that surface ocean temperature is the right approach for the dominant groups and regions. The seasonal range of SST in low latitudes is low (less than 0.5 °C), with only minor differences between the LGM and the pre-industrial, which cannot therefore explain our observation (Supplementary Fig. 6). However, the LGM climate reconstruction is still an active developing topic<sup>62</sup>. Although we include multiple realizations of the modelled LGM climate (cGENIE and HadCM3 as below) and proxy-based temperature<sup>77</sup>, the thermal optima in our study are conditional to the fidelity of these reconstructed climate states.

**LGM and pre-industrial foraminiferal thermal performance curves Quantile regression model.** We fit thermal performance curves (norm reaction) using a nonlinear quantile regression model from the R package `quantregGrowth`<sup>79</sup>. This approach has been used to estimate upper limit functions such as the Eppley curve<sup>80</sup>, which describes the exponential increase in maximum phytoplankton growth rates with temperature. However, the fitted maximum abundances of foraminifera have higher uncertainties in those undersampled regions. To quantify such uncertainty, we apply ten different models with quantile levels from the 90th to the 99th and calculate their mean and s.d. The resulting s.d. that measures the sensitivities of the models to the outlier values could provide an assessment of the sampling effort in this region (Fig. 1).

**Rendering the optimal temperature.** The fitted quantile models are then used to estimate the optimal temperature range at each age. We set half of the maximum abundance (in both the LGM and the pre-industrial pool) as the threshold. The thermal optima of species in the LGM and in the pre-industrial era are provided in Extended Data Table 1.

**Validating the relative abundance-based optimal niche.** To validate the thermal optimum based on relative abundance, we compare the species' optimal temperatures with previous estimations based on the largest body size<sup>21</sup> and the highest growth rate<sup>20</sup>. The result shows that the relative abundance-based optimal temperatures are very consistent with those estimations based on biological traits (Extended Data Table 1). Our method also provides the s.d. of the optimal temperature range, which measures the breadth of the optimal niche.

However, we caution our readers about the potential bias when using relative abundance-based optimal niches for rare species. In an extreme scenario, a rare species could have its lowest relative abundance even when it is at its highest absolute abundance. This can occur when a dominant species exists in a similar optimal niche. Nevertheless, this bias is not a substantial concern for dominant species, because their relative abundance is hardly influenced by rare species. Overall, our estimations of optimal niche for dominant species and ecogroup are robust, whereas results for species with a low abundance need to be processed with caution.

**ANOVA.** We conducted two-way ANOVAs in R (v.4.3.1)<sup>81</sup> to explain the species difference of thermal optimum from the LGM to the pre-industrial era using their symbiosis and spine trait. The full species list and their related trait attribution are provided in Supplementary Table 1.

## Reporting summary

Further information on research design is available in the Nature Portfolio Reporting Summary linked to this article.

## Data availability

The MARGO and ForCenS fossil data, in addition to the previously described<sup>77</sup> LGM temperature assimilation product, can be retrieved from <https://www.pangaea.de>. The HadISST data product is publicly available at <https://www.metoffice.gov.uk/hadobs/hadisst/>. All the CMIP6 data can be downloaded from <https://esgf-node.llnl.gov/projects/cmip6/>. The cleaned foraminifera fossil abundance and temperature data in this study are available at <https://zenodo.org/doi/10.5281/zenodo.8189768> (ref. 82). The existing pre-industrial, LGM and future cGENIE model outputs are archived in <https://zenodo.org/doi/10.5281/zenodo.8189647> (ref. 83). The reanalysed data from a previous study<sup>12</sup> are available at <https://zenodo.org/doi/10.5281/zenodo.8189772> (ref. 84). Source data are provided with this paper.

## Code availability

The cGENIE model code used in this study is available at [https://github.com/ruiying-ocean/cgenie.muffin/tree/DEV\\_Forum/](https://github.com/ruiying-ocean/cgenie.muffin/tree/DEV_Forum/) (<https://zenodo.org/doi/10.5281/zenodo.12658600>). Instructions including commands to run the models can be found in the `genie-userconfig/FORAMECOGEM/readme.txt`. Model data analyses were performed using `cgeniepy` (v.0.7.5)<sup>85</sup>. All the scripts for analyses and visualizations are stored at [https://github.com/ruiying-ocean/lgm\\_foram\\_niche](https://github.com/ruiying-ocean/lgm_foram_niche).

- Pohl, A. et al. Continental configuration controls ocean oxygenation during the Phanerozoic. *Nature* **608**, 523–527 (2022).
- Edwards, N. R. & Marsh, R. Uncertainties due to transport-parameter sensitivity in an efficient 3-D ocean-climate model. *Clim. Dyn.* **24**, 415–433 (2005).
- Marsh, R., Müller, S. A., Yool, A. & Edwards, N. R. Incorporation of the C-GOLDSTEIN efficient climate model into the GENIE framework: 'eb\_go\_gs' configurations of GENIE. *Geosci. Model Dev.* **4**, 957–992 (2011).
- Ridgwell, A. et al. Marine geochemical data assimilation in an efficient Earth System Model of global biogeochemical cycling. *Biogeosciences* **4**, 87–104 (2007).
- Davies-Barnard, T., Ridgwell, A., Singarayer, J. & Valdes, P. Quantifying the influence of the terrestrial biosphere on glacial-interglacial climate dynamics. *Clim. Past* **13**, 1381–1401 (2017).
- Albani, S. et al. Paleodust variability since the Last Glacial Maximum and implications for iron inputs to the ocean. *Geophys. Res. Lett.* **43**, 3944–3954 (2016).
- Morée, A. L. & Schwinger, J. A Last Glacial Maximum forcing dataset for ocean modelling. *Earth Syst. Sci. Data* **12**, 2971–2985 (2020).
- Kageyama, M. et al. The PMIP4 contribution to CMIP6 – Part 4: Scientific objectives and experimental design of the PMIP4-CMIP6 Last Glacial Maximum experiments and PMIP4 sensitivity experiments. *Geosci. Model Dev.* **10**, 4035–4055 (2017).
- Ödalen, M. *Model Analysis of Ocean Carbon Storage and Transport Across Climate States*. PhD thesis, Stockholm Univ. (2019).
- Bouttes, N., Paillard, D. & Roche, D. M. Impact of brine-induced stratification on the glacial carbon cycle. *Clim. Past* **6**, 575–589 (2010).
- Peterson, C. D., Lisiecki, L. E. & Stern, J. V. Deglacial whole-ocean  $\delta^{13}\text{C}$  change estimated from 480 benthic foraminiferal records. *Paleoceanography* **29**, 549–563 (2014).
- Muglia, J., Skinner, L. C. & Schmittner, A. Weak overturning circulation and high Southern Ocean nutrient utilization maximized glacial ocean carbon. *Earth Planet. Sci. Lett.* **496**, 47–56 (2018).
- Kageyama, M. et al. The PMIP4 Last Glacial Maximum experiments: preliminary results and comparison with the PMIP3 simulations. *Clim. Past* **17**, 1065–1089 (2021).
- Annan, J. D., Hargreaves, J. C. & Mairitsen, T. A new global surface temperature reconstruction for the Last Glacial Maximum. *Clim. Past* **18**, 1883–1896 (2022).
- Jonkers, L. & Kučera, M. Quantifying the effect of seasonal and vertical habitat tracking on planktonic foraminifera proxies. *Clim. Past* **13**, 573–586 (2017).
- Cao, L. et al. The role of ocean transport in the uptake of anthropogenic  $\text{CO}_2$ . *Biogeosciences* **6**, 375–390 (2009).
- Mahowald, N. M. et al. Change in atmospheric mineral aerosols in response to climate: last glacial period, preindustrial, modern, and doubled carbon dioxide climates. *J. Geophys. Res.* **111**, D10202 (2006).
- Morice, C. P. et al. An updated assessment of near-surface temperature change from 1850: the HadCRUT5 data set. *J. Geophys. Res. Atmos.* **126**, e2019JD032361 (2021).
- Tittensor, D. P. et al. Next-generation ensemble projections reveal higher climate risks for marine ecosystems. *Nat. Clim. Change* **11**, 973–981 (2021).
- Michaels, A. F., Caron, D. A., Swanberg, N. R., Howse, F. A. & Michaels, C. M. Planktonic sarcodines (Acantharia, Radiolaria, Foraminifera) in surface waters near Bermuda: abundance, biomass and vertical flux. *J. Plankton Res.* **17**, 131–163 (1995).
- Fraille, I. et al. Modeling the seasonal distribution of planktonic foraminifera during the Last Glacial Maximum. *Paleoceanography* **24**, PA2216 (2009).
- Siccha, M. & Kucera, M. ForCenS, a curated database of planktonic foraminifera census counts in marine surface sediment samples. *Sci. Data* **4**, 170109 (2017).
- Kucera, M., Rosell-Melé, A., Schneider, R., Waelbroeck, C. & Weinelt, M. Multiproxy approach for the reconstruction of the glacial ocean surface (MARGO). *Quat. Sci. Rev.* **24**, 813–819 (2005).

# Article

72. Brummer, G.-J. A. & Kučera, M. Taxonomic review of living planktonic foraminifera. *J. Micropalaeontol.* **41**, 29–74 (2022).
73. Takagi, H. et al. Characterizing photosymbiosis in modern planktonic foraminifera. *Biogeosciences* **16**, 3377–3396 (2019).
74. Schiebel, R. & Hemleben, C. *Planktic Foraminifers in the Modern Ocean* (Springer Berlin, 2017).
75. Huber, B. T. et al. Pforams@microtax: A new online taxonomic database for planktonic foraminifera. *Micropaleontology* **62**, 429–438 (2016).
76. Rayner, N. A. et al. Global analyses of sea surface temperature, sea ice, and night marine air temperature since the late nineteenth century. *J. Geophys. Res.* **108**, 4407 (2003).
77. Tierney, J. E. et al. Glacial cooling and climate sensitivity revisited. *Nature* **584**, 569–573 (2020).
78. Rebotim, A. et al. Factors controlling the depth habitat of planktonic foraminifera in the subtropical eastern North Atlantic. *Biogeosciences* **14**, 827–859 (2017).
79. Muggeo, V. M. R., Torretta, F., Eilers, P., Sciandra, M. & Attanasio, M. Multiple smoothing parameters selection in additive regression quantiles. *Stat. Model.* **21**, 428–448 (2021).
80. Kremer, C. T., Thomas, M. K. & Litchman, E. Temperature- and size-scaling of phytoplankton population growth rates: reconciling the Eppley curve and the metabolic theory of ecology. *Limnol. Oceanogr.* **62**, 1658–1670 (2017).
81. R Core Team. *R: A Language and Environment for Statistical Computing*. <https://www.R-project.org/> (R Foundation for Statistical Computing, 2023).
82. Ying, R. ruiying-ocean/lgm\_foram\_census: Foraminifera abundance data in the LGM/PI. *Zenodo* <https://zenodo.org/doi/10.5281/zenodo.8189768> (2024).
83. Ying, R., Monteiro, F. M., Wilson, J. D. & Schmidt, D. N. Modelled planktic foraminifera from LGM to future (ForamEcoGENIE). *Zenodo* <https://zenodo.org/doi/10.5281/zenodo.8189647> (2024).
84. Ying, R. ruiying-ocean/quanternary\_foram\_niche: Foraminifera optimal niche reanalysis based on Antell et al. (2021) data. *Zenodo* <https://zenodo.org/doi/10.5281/zenodo.8189772> (2024).
85. Ying, R. cgeniepy: a Python package for analysing cGENIE Earth System Model output. Preprint at <https://doi.org/10.21203/rs.3.rs-3967633/v1> (2024).

**Acknowledgements** The authors thank P. J. Valdes for providing HadCM3 data to configure the cGENIE model. R.Y. is funded by the China Scholarship Council (202006380070) and the Bob Savage Memorial Funding. R.Y. acknowledges R. Barrett for proofreading and the JASMIN facilities to access CMIP data. F.M.M. (NE/X001261/1 and NE/V01823X/1) and D.N.S. (NE/PO19439/1) thank the Natural Environment Research Council (NERC) for funding. J.D.W. acknowledges support from the AXA Research Fund.

**Author contributions** R.Y., F.M.M. and D.N.S. conceived the study. R.Y. performed all model simulations, data compilation, analysis and visualization. F.M.M., J.D.W. and D.N.S. supervised the project. M.Ö. provided the raw LGM model configuration. R.Y., F.M.M. and D.N.S. wrote and edited the manuscript. All authors reviewed the manuscript.

**Competing interests** The authors declare no competing interests.

#### Additional information

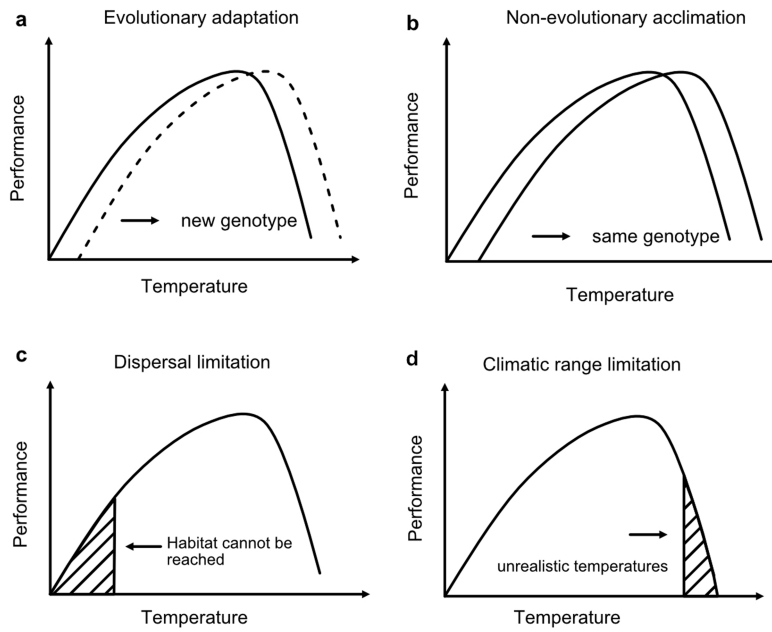
**Supplementary information** The online version contains supplementary material available at <https://doi.org/10.1038/s41586-024-08029-0>.

**Correspondence and requests for materials** should be addressed to Rui Ying.

**Peer review information** *Nature* thanks Moriaki Yasuhara and the other, anonymous, reviewer(s) for their contribution to the peer review of this work. Peer reviewer reports are available.

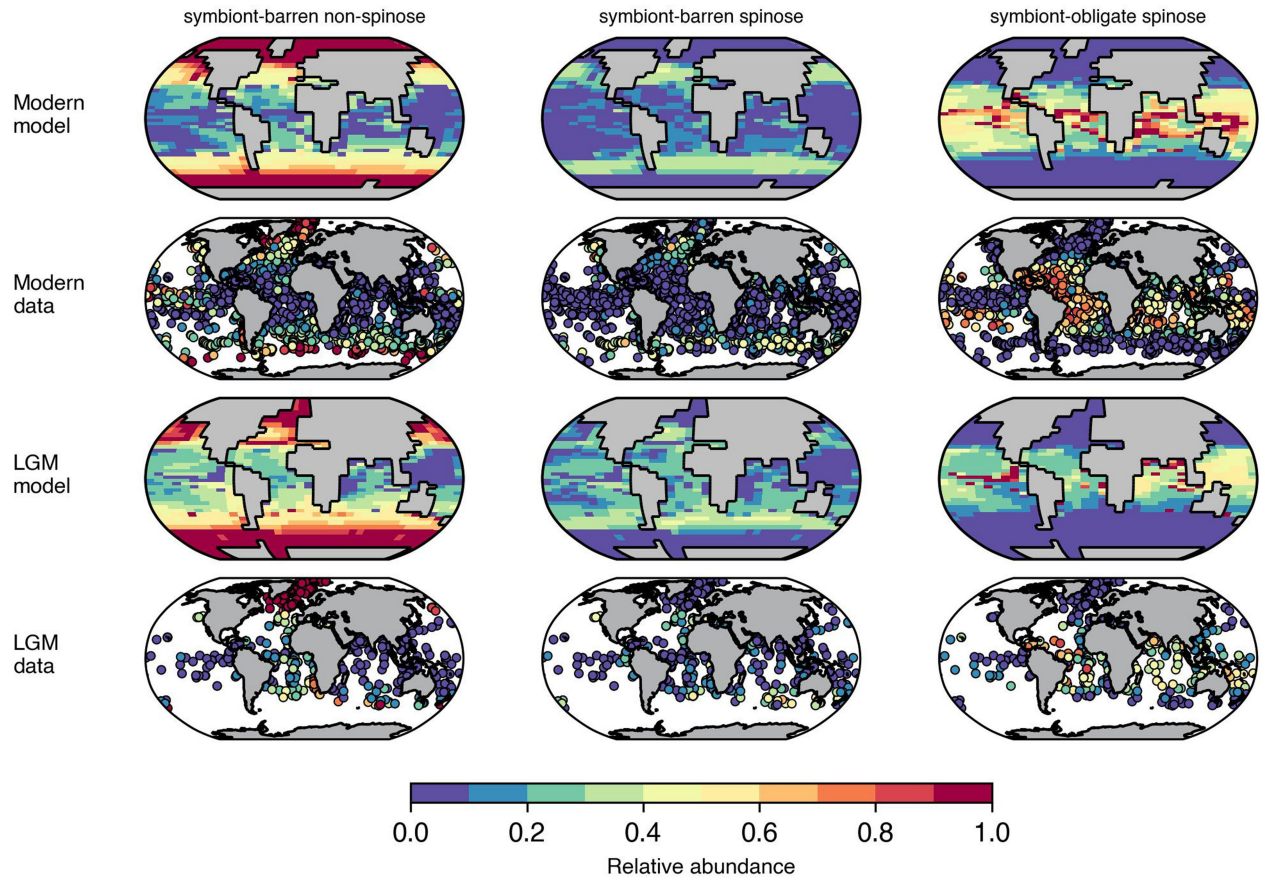
**Reprints and permissions information** is available at <http://www.nature.com/reprints>.





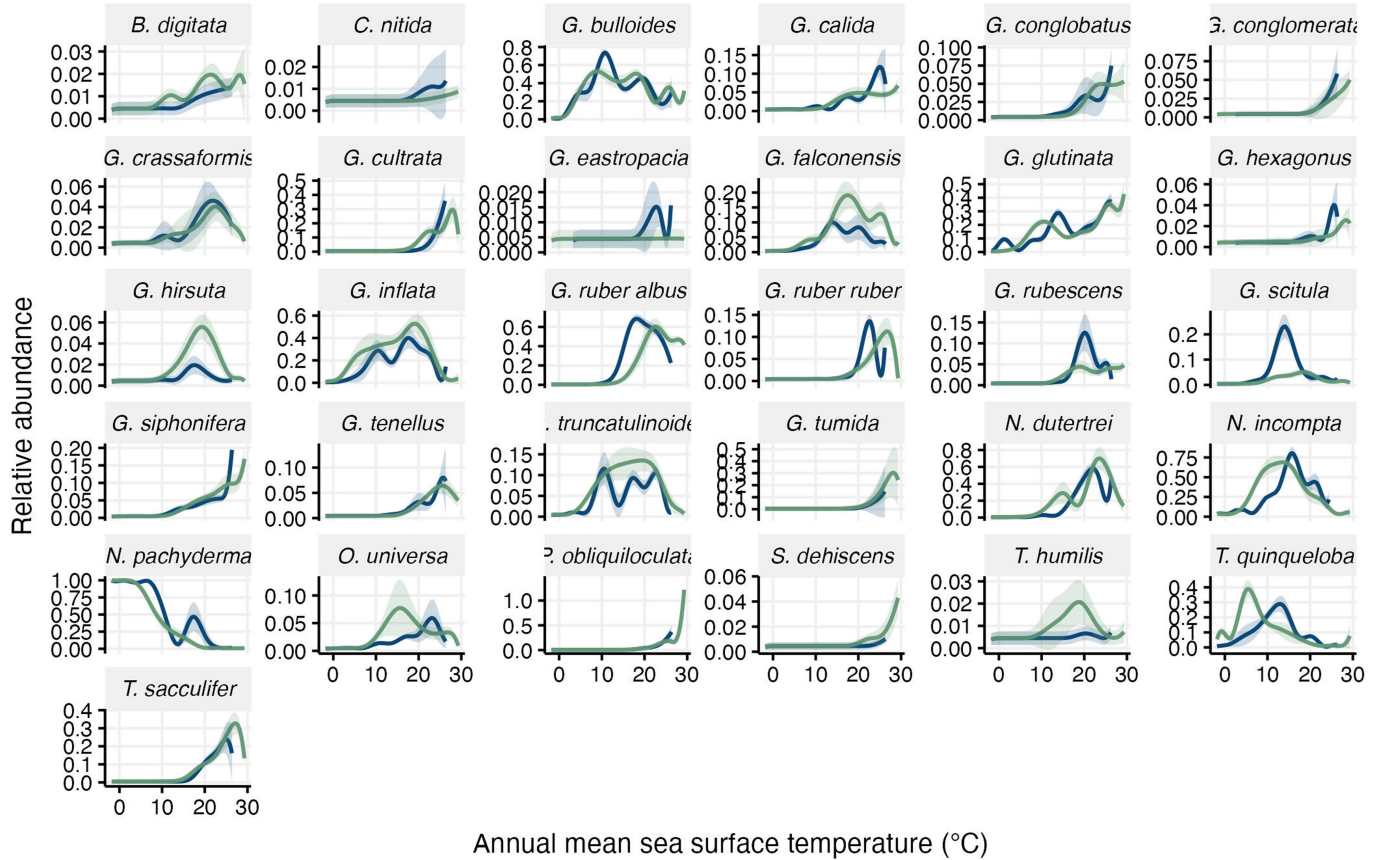
**Extended Data Fig. 1 | Schematic illustration of realized thermal niche change (the thermal performance function) under different causes. a–d.** The adaptive responses including) evolution (defined by generation of new genotypes) (a) and acclimatization (non-evolutionary plasticity) (b) change the thermal performance function. By contrast, dispersal limitation

where some species cannot reach a particular geographical area (hatched area) (c) or climatic range limitation where the temperature range is not available at a given time (e.g., temperatures above 25 °C during the LGM) (d) only affect the range of realized thermal niche.



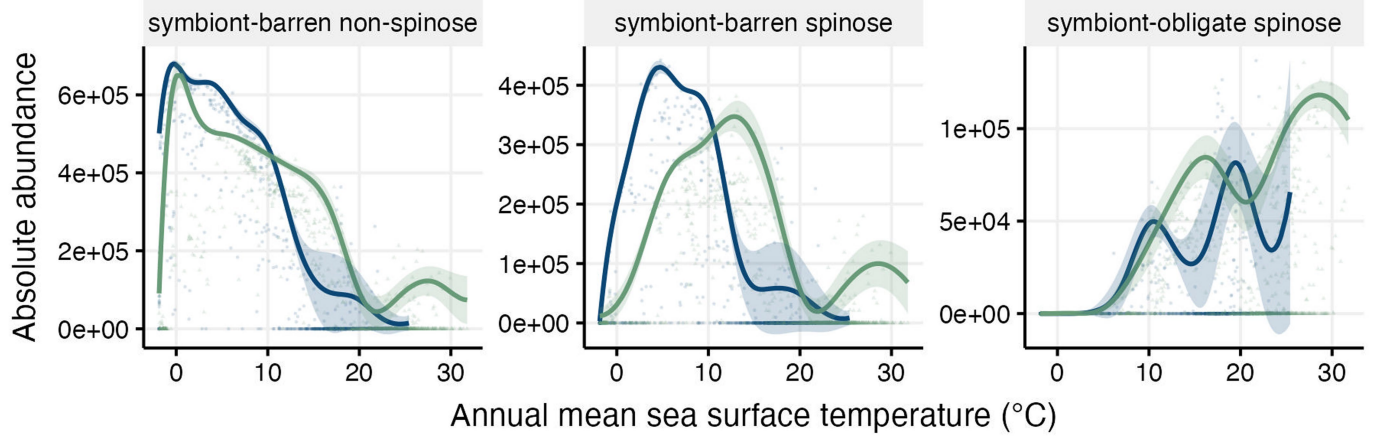
**Extended Data Fig. 2 | Model and fossil data comparison of relative abundance from sediment cores for the three foraminiferal ecogroups in the pre-industrial era and the LGM.** The model captures both the observed habitat contraction of the symbiont-barren groups from LGM to pre-industrial

with a broader geographic distribution in the LGM and the increasing relative abundance of the symbiont-obligate group in the modern ocean compared to the LGM.

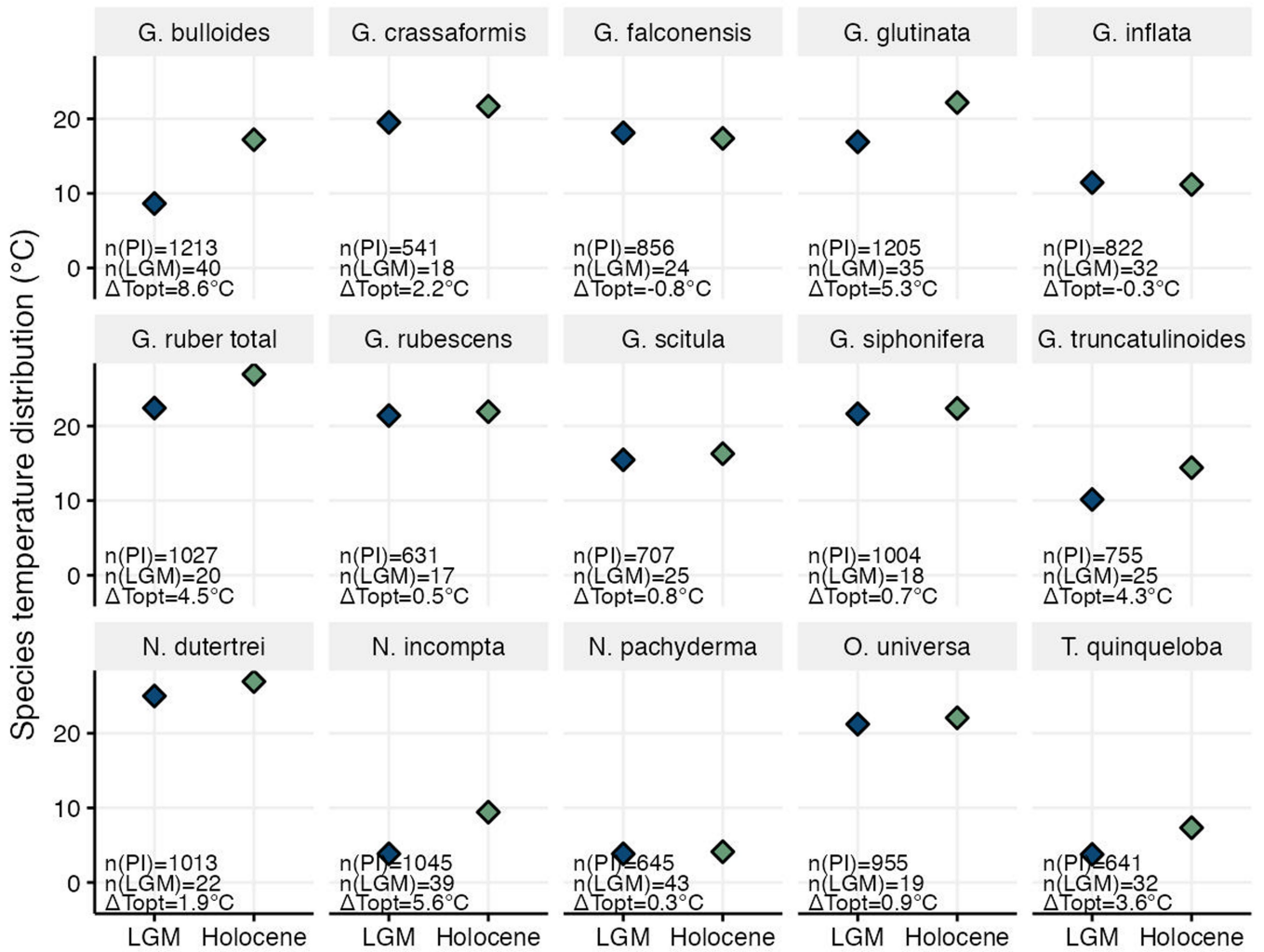


**Extended Data Fig. 3 | Species-level thermal performance curves for the LGM and the pre-industrial age.** Data as in Fig. 1 (LGM (19–21 ka), blue; pre-industrial age (0 ka), green) but here disaggregated at species level. The full species name and related ecogroup can be found in Supplementary Table 1. Notable species showing changes in the thermal performance interpreted as

acclimatization include the tropical symbiont-bearing taxa *T. sacculifer*, *G. ruber ruber*, *G. ruber albus*, and *N. dutertrei* and *N. incompta*. Note: the y scale is set different for each species to highlight patterns. The shaded area represents the standard deviation of the 90–99th quantile regression model results.

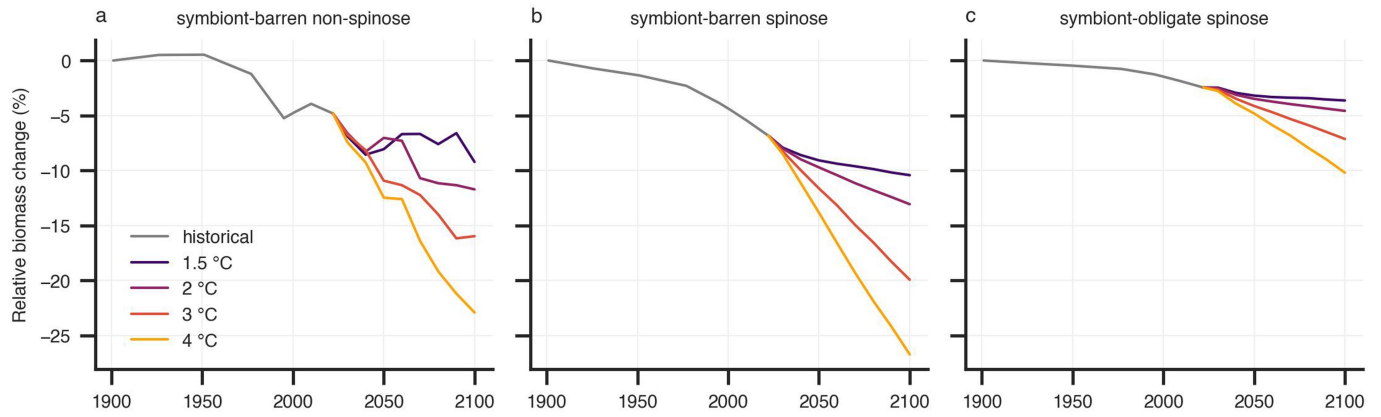


**Extended Data Fig. 4 | Modelled foraminiferal thermal performance curve based on the absolute abundance of cGENIE output.** The consistency between absolute abundance and relative abundance-based results (Fig. 1) indicates that niche shift was not caused by community compositional change only.



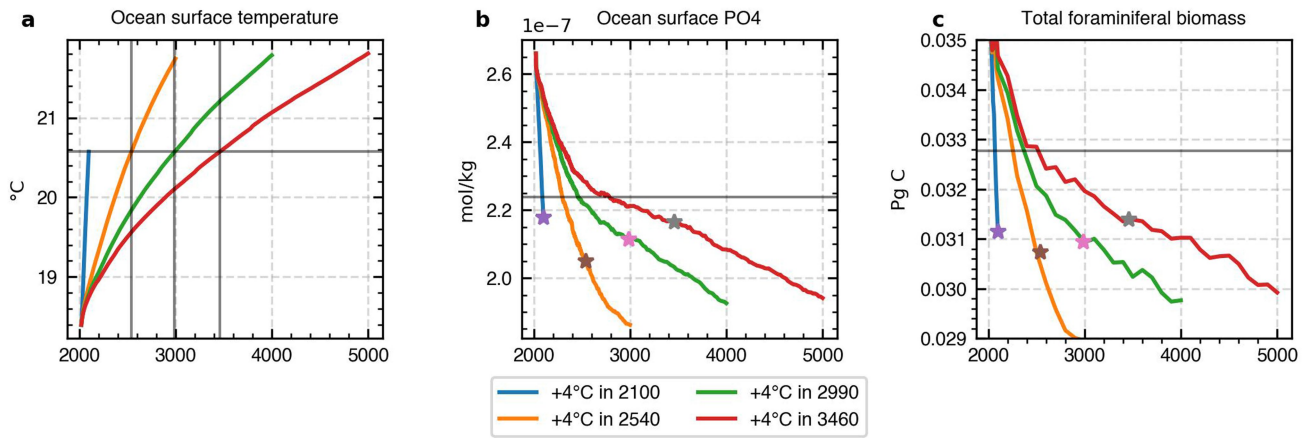
**Extended Data Fig. 5 | Foraminiferal thermal optimal niche in the LGM and Holocene using presence- and absence-based foraminifera occurrences and vertically resolved temperature data.** The optimal temperature of the species, defined as the highest occurrence probability, is marked by diamond

for both LGM (20 ka bin, left) and Holocene (4 ka bin, right). The annotated text shows the optimal temperature change (Holocene-LGM) for each species and the number of presence data to reconstruct the optimal niche. The vertically resolved temperature data are from a previous study<sup>12</sup>.



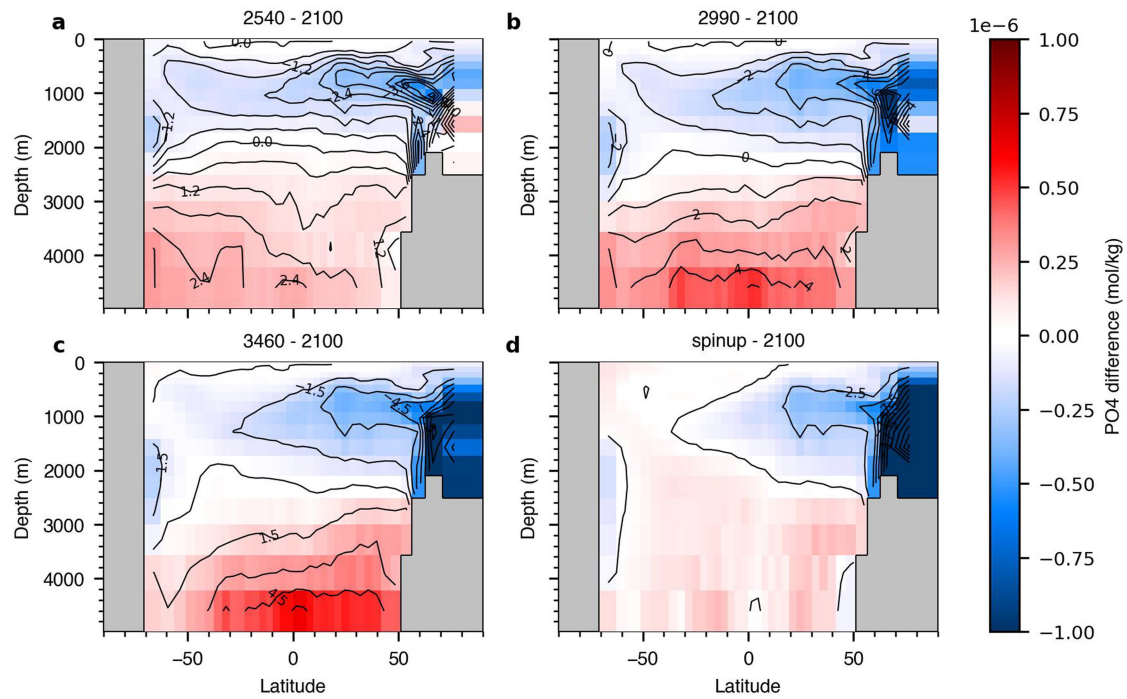
**Extended Data Fig. 6 | Projected globally integrated carbon biomass (standing stock) of each foraminifera ecogroup from 2022 to 2100 in response to four different warming scenarios. a, b,** The biomasses of symbiont-barren non-spinose (a) and symbiont-barren spinose (b) foraminifera

show a reduction of 10–27% relative to the 1900–1950 average. **c,** By contrast, symbiont-obligate foraminifera are the most resilient to warming with 4–10% reduction depending on the warming pathways. Note that symbiont-barren foraminifera drive 77% of the total foraminifera change.



**Extended Data Fig. 7 | Model responses of surface mean nutrient (shown here as PO<sub>4</sub>) and total foraminifera biomass to a 4 °C warming under different warming rates.** **a**, The ocean surface temperature responses to CO<sub>2</sub> emission at different rates. The grey lines mark the model years with the same warming magnitudes (4 °C warming relative to the 1900–1950 average) for different model runs. **b**, The surface PO<sub>4</sub> concentration changes in response to warmings. **c**, The total foraminiferal biomass in each model experiments.

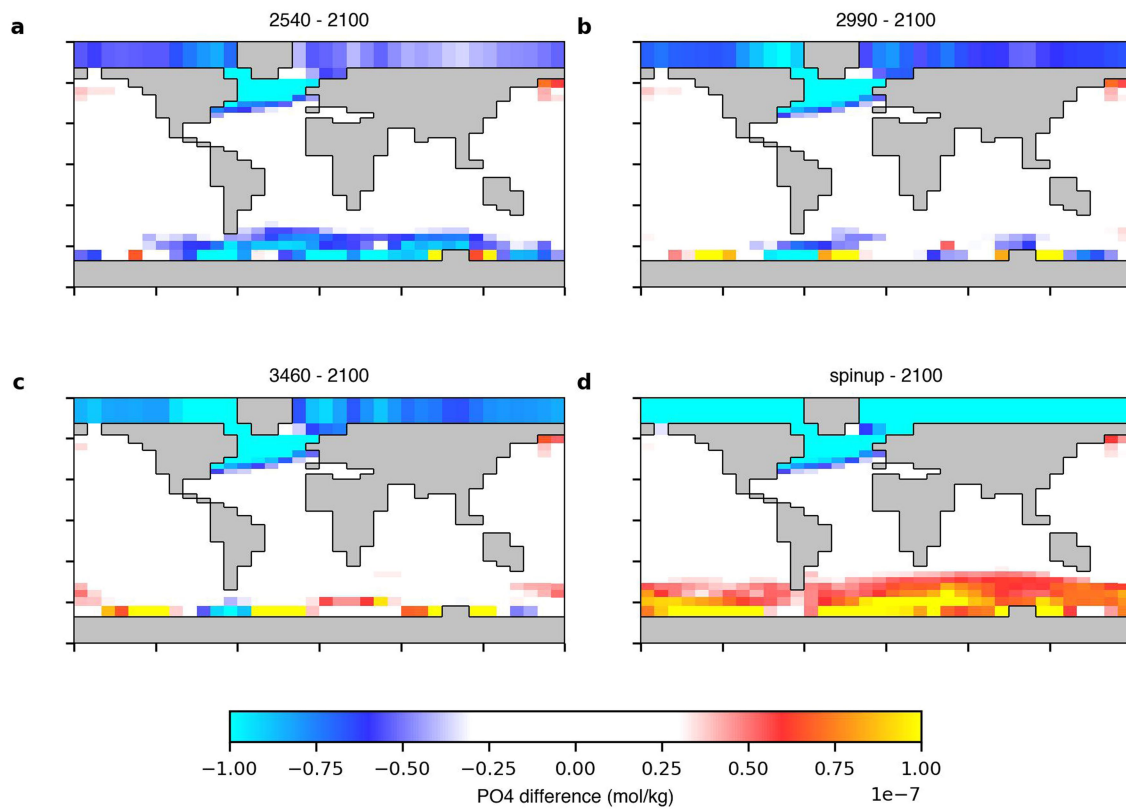
The stars in **b,c** represent model years when the ocean surface reaches the same warming magnitude at different rates. The horizontal lines in subplots **b,c** show the state in surface nutrient and foraminifera biomass under fully equilibrium state. This figure shows that decreasing the warming rate damps any resulting ocean stratification and associated reduction of surface nutrient supply.



**Extended Data Fig. 8 | The global zonal mean PO<sub>4</sub> anomaly in the slow-warming scenarios relative to the fastest warming scenario. a-d.** As in Extended Data Fig. 7, each panel shows the nutrient distribution difference at different warming rate despite the same warming magnitude. Compared to the

fastest warming scenario (reached in 2100), the slower warming rates (reached in 2540, 2990, 3460, and in a steady-state model) allow more nutrients to be delivered to the surface.





**Extended Data Fig. 9 | The spatial distribution of surface PO<sub>4</sub> concentration difference between slow and fast warming experiments.** As shown in the Extended Data Fig. 8, with a gradually slower emission rate (from **a** to **d**), there

is more nutrient availability in the Southern Ocean under the same surface ocean warming level. The North Atlantic, however, keeps being isolated and nutrient-depleted.

# Article

**Extended Data Table 1 | The mean thermal optimum\* values and standard deviation for foraminifera species (in degrees Celsius) for the LGM and pre-industrial age**

Species	Mean $\pm$ S.D. (LGM)	Mean $\pm$ S.D. (PI)	Size-based estimation (PI) <sup>†</sup>	Culture data (PI) <sup>‡</sup>
<i>B. digitata</i>	22.5 $\pm$ 1.6	23.9 $\pm$ 4.3		
<i>C. nitida</i>	22.6 $\pm$ 1.5	27.4 $\pm$ 0.8		
<i>G. bulloides</i>	15.3 $\pm$ 3.5	14.4 $\pm$ 4.3	10.5, 23.8	9–25
<i>G. calida</i>	23.5 $\pm$ 0.8	28.9 $\pm$ 0.2		
<i>G. conglobatus</i>	25.4 $\pm$ 0.4	26.1 $\pm$ 1.9	26.9	
<i>G. conglomerata</i>	25.0 $\pm$ 0.5	27.4 $\pm$ 0.8		
<i>G. crassaformis</i>	21.8 $\pm$ 2.2	23.4 $\pm$ 2.5		
<i>G. cultrata</i>	25.1 $\pm$ 0.4	27.3 $\pm$ 0.8	27.7	
<i>G. falconensis</i>	14.0 $\pm$ 0.3	22.0 $\pm$ 3.9		
<i>G. glutinata</i>	19.0 $\pm$ 4.9	25.4 $\pm$ 4.3		
<i>G. hexagonus</i>	25.0 $\pm$ 0.5	27.9 $\pm$ 0.6		
<i>G. hirsuta</i>	NA	19.4 $\pm$ 2.4	22.8	
<i>G. inflata</i>	18.1 $\pm$ 3.2	16.3 $\pm$ 4.7	18.2, 27.9	
<i>G. ruber albus</i>	20.1 $\pm$ 3.1	25.4 $\pm$ 2.6	27.5	20-29
<i>G. ruber ruber</i>	22.7 $\pm$ 0.8	26.4 $\pm$ 1.3	27.5	20-29
<i>G. rubescens</i>	20.0 $\pm$ 1.5	NA		
<i>G. scitula</i>	14.1 $\pm$ 1.3	NA		
<i>G. siphonifera</i>	25.8 $\pm$ 0.3	27.3 $\pm$ 0.9		20-29
<i>G. tenellus</i>	24.6 $\pm$ 0.7	26.1 $\pm$ 1.8		
<i>G. truncatulinoides</i>	19.4 $\pm$ 3.8	17.8 $\pm$ 4.5	19.8	
<i>G. tumida</i>	NA	27.1 $\pm$ 1.0	28.4	
<i>N. dutertrei</i>	22.1 $\pm$ 1.4	24.9 $\pm$ 1.8		8–25
<i>N. incompta</i>	16.0 $\pm$ 2.3	13.6 $\pm$ 3.4	11.4	6-20
<i>N. pachyderma</i>	3.0 $\pm$ 3.9	4.4 $\pm$ 2.7	0.3	<5
<i>O. universa</i>	22.9 $\pm$ 0.9	17.0 $\pm$ 2.7	22.4	20-29
<i>P. obliquiloculata</i>	NA	28.9 $\pm$ 0.2		
<i>S. dehiscens</i>	NA	28.0 $\pm$ 0.5		
<i>T. humilis</i>	NA	18.3 $\pm$ 2.7		
<i>T. quinqueloba</i>	13.2 $\pm$ 1.3	6.2 $\pm$ 1.7		
<i>T. sacculifer</i>	23.5 $\pm$ 0.8	26.5 $\pm$ 1.5	27.2	20-29

\*The thermal optimum is defined as the temperature range with more than 50% maximum relative abundance of both LGM and pre-industrial (PI) age. The NA in this table suggests that some taxa satisfy the optimal condition.

<sup>†</sup>The optimal temperatures defined as the maximum body size where available in Schmidt et al.<sup>21</sup>. The *G. ruber* in this study include two subspecies, which are separated in our study.

<sup>‡</sup>The optimal temperatures defined as the maximum growth rate where available in Lombard et al.<sup>20</sup>.

## Reporting Summary

Nature Portfolio wishes to improve the reproducibility of the work that we publish. This form provides structure for consistency and transparency in reporting. For further information on Nature Portfolio policies, see our [Editorial Policies](#) and the [Editorial Policy Checklist](#).

### Statistics

For all statistical analyses, confirm that the following items are present in the figure legend, table legend, main text, or Methods section.

n/a Confirmed

- The exact sample size ( $n$ ) for each experimental group/condition, given as a discrete number and unit of measurement
- A statement on whether measurements were taken from distinct samples or whether the same sample was measured repeatedly
- The statistical test(s) used AND whether they are one- or two-sided  
*Only common tests should be described solely by name; describe more complex techniques in the Methods section.*
- A description of all covariates tested
- A description of any assumptions or corrections, such as tests of normality and adjustment for multiple comparisons
- A full description of the statistical parameters including central tendency (e.g. means) or other basic estimates (e.g. regression coefficient) AND variation (e.g. standard deviation) or associated estimates of uncertainty (e.g. confidence intervals)
- For null hypothesis testing, the test statistic (e.g.  $F$ ,  $t$ ,  $r$ ) with confidence intervals, effect sizes, degrees of freedom and  $P$  value noted  
*Give  $P$  values as exact values whenever suitable.*
- For Bayesian analysis, information on the choice of priors and Markov chain Monte Carlo settings
- For hierarchical and complex designs, identification of the appropriate level for tests and full reporting of outcomes
- Estimates of effect sizes (e.g. Cohen's  $d$ , Pearson's  $r$ ), indicating how they were calculated

*Our web collection on [statistics for biologists](#) contains articles on many of the points above.*

### Software and code

Policy information about [availability of computer code](#)

Data collection

No software was used for data collection.

Data analysis

We use codes in [https://github.com/ruiying-ocean/lgm\\_foram\\_census](https://github.com/ruiying-ocean/lgm_foram_census) to find foraminifera living sea surface temperature. The codes to analyse and visualise the produced data are stored in [https://github.com/ruiying-ocean/lgm\\_foram\\_niche](https://github.com/ruiying-ocean/lgm_foram_niche). For the cGENIE data analysis, I used Python package [cgeniepy v0.7.5](https://github.com/ruiying-ocean/cgeniepy) (<https://github.com/ruiying-ocean/cgeniepy>). The codes to reanalyse the data of Antell et al. (2021) are stored in [https://github.com/ruiying-ocean/quanternary\\_foram\\_niche](https://github.com/ruiying-ocean/quanternary_foram_niche).

For manuscripts utilizing custom algorithms or software that are central to the research but not yet described in published literature, software must be made available to editors and reviewers. We strongly encourage code deposition in a community repository (e.g. GitHub). See the Nature Portfolio [guidelines for submitting code & software](#) for further information.

### Data

Policy information about [availability of data](#)

All manuscripts must include a [data availability statement](#). This statement should provide the following information, where applicable:

- Accession codes, unique identifiers, or web links for publicly available datasets
- A description of any restrictions on data availability
- For clinical datasets or third party data, please ensure that the statement adheres to our [policy](#)

The MARGO and ForCenS fossil data, in addition to the Tierney et al. (2020) LGM temperature assimilation product, can be retrieved from <https://www.pangaea.de>.

The HadISST data product is publicly available at <https://www.metoffice.gov.uk/hadobs/hadisst/>.

All the CMIP6 data can be downloaded from <https://esgf-node.llnl.gov/projects/cmip6/>.

The cleaned foraminifera fossil abundance and temperature data in this study are available at <https://zenodo.org/doi/10.5281/zenodo.8189768>. The existing pre-industrial, LGM and future cGENIE model outputs are archived in <https://zenodo.org/doi/10.5281/zenodo.8189647>. The reanalysed data of Antell et al. (2021) is available at <https://zenodo.org/doi/10.5281/zenodo.8189772>.

## Research involving human participants, their data, or biological material

Policy information about studies with [human participants or human data](#). See also policy information about [sex, gender \(identity/presentation\), and sexual orientation](#) and [race, ethnicity and racism](#).

Reporting on sex and gender	N/A
Reporting on race, ethnicity, or other socially relevant groupings	N/A
Population characteristics	N/A
Recruitment	N/A
Ethics oversight	N/A

Note that full information on the approval of the study protocol must also be provided in the manuscript.

## Field-specific reporting

Please select the one below that is the best fit for your research. If you are not sure, read the appropriate sections before making your selection.

Life sciences       Behavioural & social sciences       Ecological, evolutionary & environmental sciences

For a reference copy of the document with all sections, see [nature.com/documents/nr-reporting-summary-flat.pdf](https://nature.com/documents/nr-reporting-summary-flat.pdf)

## Life sciences study design

All studies must disclose on these points even when the disclosure is negative.

Sample size	<i>Describe how sample size was determined, detailing any statistical methods used to predetermine sample size OR if no sample-size calculation was performed, describe how sample sizes were chosen and provide a rationale for why these sample sizes are sufficient.</i>
Data exclusions	<i>Describe any data exclusions. If no data were excluded from the analyses, state so OR if data were excluded, describe the exclusions and the rationale behind them, indicating whether exclusion criteria were pre-established.</i>
Replication	<i>Describe the measures taken to verify the reproducibility of the experimental findings. If all attempts at replication were successful, confirm this OR if there are any findings that were not replicated or cannot be reproduced, note this and describe why.</i>
Randomization	<i>Describe how samples/organisms/participants were allocated into experimental groups. If allocation was not random, describe how covariates were controlled OR if this is not relevant to your study, explain why.</i>
Blinding	<i>Describe whether the investigators were blinded to group allocation during data collection and/or analysis. If blinding was not possible, describe why OR explain why blinding was not relevant to your study.</i>

## Behavioural & social sciences study design

All studies must disclose on these points even when the disclosure is negative.

Study description	<i>Briefly describe the study type including whether data are quantitative, qualitative, or mixed-methods (e.g. qualitative cross-sectional, quantitative experimental, mixed-methods case study).</i>
Research sample	<i>State the research sample (e.g. Harvard university undergraduates, villagers in rural India) and provide relevant demographic information (e.g. age, sex) and indicate whether the sample is representative. Provide a rationale for the study sample chosen. For studies involving existing datasets, please describe the dataset and source.</i>
Sampling strategy	<i>Describe the sampling procedure (e.g. random, snowball, stratified, convenience). Describe the statistical methods that were used to predetermine sample size OR if no sample-size calculation was performed, describe how sample sizes were chosen and provide a rationale for why these sample sizes are sufficient. For qualitative data, please indicate whether data saturation was considered, and what criteria were used to decide that no further sampling was needed.</i>

Data collection	<i>Provide details about the data collection procedure, including the instruments or devices used to record the data (e.g. pen and paper, computer, eye tracker, video or audio equipment) whether anyone was present besides the participant(s) and the researcher, and whether the researcher was blind to experimental condition and/or the study hypothesis during data collection.</i>
Timing	<i>Indicate the start and stop dates of data collection. If there is a gap between collection periods, state the dates for each sample cohort.</i>
Data exclusions	<i>If no data were excluded from the analyses, state so OR if data were excluded, provide the exact number of exclusions and the rationale behind them, indicating whether exclusion criteria were pre-established.</i>
Non-participation	<i>State how many participants dropped out/declined participation and the reason(s) given OR provide response rate OR state that no participants dropped out/declined participation.</i>
Randomization	<i>If participants were not allocated into experimental groups, state so OR describe how participants were allocated to groups, and if allocation was not random, describe how covariates were controlled.</i>

## Ecological, evolutionary & environmental sciences study design

All studies must disclose on these points even when the disclosure is negative.

Study description	We study the global thermal performances of planktic foraminifera under different climate states using mechanistic models and fossil observations.
Research sample	Fossil samples (species, abundance, latitude and longitude) of planktic foraminifera
Sampling strategy	All global fossil samples where relative abundance is known
Data collection	We collect fossil foraminifera data from existing MARGO and ForCenS projects. Corresponding temperature data are from HadISST and Tierney et al. (2020).
Timing and spatial scale	Global scale in the Last Glacial Maximum and Pre-industrial age
Data exclusions	Multiple morphospecies will be merged in abundance (e.g., <i>T. sacculifer</i> sac and <i>T. sacculifer</i> without sac)
Reproducibility	All the data and codes are provided for promoting reproducibility. Specific visualisation codes are shared in <a href="https://github.com/ruiying-ocean/lgm_foram_niche">https://github.com/ruiying-ocean/lgm_foram_niche</a> .
Randomization	Not applicable
Blinding	Not applicable as life sciences experiments

Did the study involve field work?  Yes  No

## Field work, collection and transport

Field conditions	<i>Describe the study conditions for field work, providing relevant parameters (e.g. temperature, rainfall).</i>
Location	<i>State the location of the sampling or experiment, providing relevant parameters (e.g. latitude and longitude, elevation, water depth).</i>
Access & import/export	<i>Describe the efforts you have made to access habitats and to collect and import/export your samples in a responsible manner and in compliance with local, national and international laws, noting any permits that were obtained (give the name of the issuing authority, the date of issue, and any identifying information).</i>
Disturbance	<i>Describe any disturbance caused by the study and how it was minimized.</i>

## Reporting for specific materials, systems and methods

We require information from authors about some types of materials, experimental systems and methods used in many studies. Here, indicate whether each material, system or method listed is relevant to your study. If you are not sure if a list item applies to your research, read the appropriate section before selecting a response.

## Materials & experimental systems

## Methods

- n/a  Involved in the study
- Antibodies
- Eukaryotic cell lines
- Palaeontology and archaeology
- Animals and other organisms
- Clinical data
- Dual use research of concern
- Plants

- n/a  Involved in the study
- ChIP-seq
- Flow cytometry
- MRI-based neuroimaging

## Antibodies

Antibodies used

Validation

## Eukaryotic cell lines

Policy information about [cell lines and Sex and Gender in Research](#)

Cell line source(s)

Authentication

Mycoplasma contamination

Commonly misidentified lines (See [ICLAC](#) register)

## Palaeontology and Archaeology

Specimen provenance

Specimen deposition

Dating methods

Tick this box to confirm that the raw and calibrated dates are available in the paper or in Supplementary Information.

Ethics oversight

Note that full information on the approval of the study protocol must also be provided in the manuscript.

## Animals and other research organisms

Policy information about [studies involving animals](#); [ARRIVE guidelines](#) recommended for reporting animal research, and [Sex and Gender in Research](#)

Laboratory animals

Wild animals

Reporting on sex

numbers in this Reporting Summary. Please state if this information has not been collected. Report sex-based analyses where performed, justify reasons for lack of sex-based analysis.

**Field-collected samples** For laboratory work with field-collected samples, describe all relevant parameters such as housing, maintenance, temperature, photoperiod and end-of-experiment protocol OR state that the study did not involve samples collected from the field.

**Ethics oversight** Identify the organization(s) that approved or provided guidance on the study protocol, OR state that no ethical approval or guidance was required and explain why not.

Note that full information on the approval of the study protocol must also be provided in the manuscript.

## Clinical data

Policy information about [clinical studies](#)

All manuscripts should comply with the ICMJE [guidelines for publication of clinical research](#) and a completed [CONSORT checklist](#) must be included with all submissions.

**Clinical trial registration** Provide the trial registration number from [ClinicalTrials.gov](#) or an equivalent agency.

**Study protocol** Note where the full trial protocol can be accessed OR if not available, explain why.

**Data collection** Describe the settings and locales of data collection, noting the time periods of recruitment and data collection.

**Outcomes** Describe how you pre-defined primary and secondary outcome measures and how you assessed these measures.

## Dual use research of concern

Policy information about [dual use research of concern](#)

### Hazards

Could the accidental, deliberate or reckless misuse of agents or technologies generated in the work, or the application of information presented in the manuscript, pose a threat to:

- | No                       | Yes                      |                            |
|--------------------------|--------------------------|----------------------------|
| <input type="checkbox"/> | <input type="checkbox"/> | Public health              |
| <input type="checkbox"/> | <input type="checkbox"/> | National security          |
| <input type="checkbox"/> | <input type="checkbox"/> | Crops and/or livestock     |
| <input type="checkbox"/> | <input type="checkbox"/> | Ecosystems                 |
| <input type="checkbox"/> | <input type="checkbox"/> | Any other significant area |

### Experiments of concern

Does the work involve any of these experiments of concern:

- | No                       | Yes                      |   |
|--------------------------|--------------------------|---|
| <input type="checkbox"/> | <input type="checkbox"/> | Demonstrate how to render a vaccine ineffective                             |
| <input type="checkbox"/> | <input type="checkbox"/> | Confer resistance to therapeutically useful antibiotics or antiviral agents |
| <input type="checkbox"/> | <input type="checkbox"/> | Enhance the virulence of a pathogen or render a nonpathogen virulent        |
| <input type="checkbox"/> | <input type="checkbox"/> | Increase transmissibility of a pathogen                                     |
| <input type="checkbox"/> | <input type="checkbox"/> | Alter the host range of a pathogen  |
| <input type="checkbox"/> | <input type="checkbox"/> | Enable evasion of diagnostic/detection modalities                           |
| <input type="checkbox"/> | <input type="checkbox"/> | Enable the weaponization of a biological agent or toxin                     |
| <input type="checkbox"/> | <input type="checkbox"/> | Any other potentially harmful combination of experiments and agents         |

## Plants

**Seed stocks** Report on the source of all seed stocks or other plant material used. If applicable, state the seed stock centre and catalogue number. If plant specimens were collected from the field, describe the collection location, date and sampling procedures.

**Novel plant genotypes** Describe the methods by which all novel plant genotypes were produced. This includes those generated by transgenic approaches, gene editing, chemical/radiation-based mutagenesis and hybridization. For transgenic lines, describe the transformation method, the number of independent lines analyzed and the generation upon which experiments were performed. For gene-edited lines, describe the editor used, the endogenous sequence targeted for editing, the targeting guide RNA sequence (if applicable) and how the editor

was applied.

## Authentication

Describe any authentication procedures for each seed stock used or novel genotype generated. Describe any experiments used to assess the effect of a mutation and, where applicable, how potential secondary effects (e.g. second site T-DNA insertions, mosaicism, off-target gene editing) were examined.

## ChIP-seq

### Data deposition

- Confirm that both raw and final processed data have been deposited in a public database such as [GEO](#).
- Confirm that you have deposited or provided access to graph files (e.g. BED files) for the called peaks.

#### Data access links

May remain private before publication.

For "Initial submission" or "Revised version" documents, provide reviewer access links. For your "Final submission" document, provide a link to the deposited data.

#### Files in database submission

Provide a list of all files available in the database submission.

#### Genome browser session

(e.g. [UCSC](#))

Provide a link to an anonymized genome browser session for "Initial submission" and "Revised version" documents only, to enable peer review. Write "no longer applicable" for "Final submission" documents.

### Methodology

#### Replicates

Describe the experimental replicates, specifying number, type and replicate agreement.

#### Sequencing depth

Describe the sequencing depth for each experiment, providing the total number of reads, uniquely mapped reads, length of reads and whether they were paired- or single-end.

#### Antibodies

Describe the antibodies used for the ChIP-seq experiments; as applicable, provide supplier name, catalog number, clone name, and lot number.

#### Peak calling parameters

Specify the command line program and parameters used for read mapping and peak calling, including the ChIP, control and index files used.

#### Data quality

Describe the methods used to ensure data quality in full detail, including how many peaks are at FDR 5% and above 5-fold enrichment.

#### Software

Describe the software used to collect and analyze the ChIP-seq data. For custom code that has been deposited into a community repository, provide accession details.

## Flow Cytometry

### Plots

Confirm that:

- The axis labels state the marker and fluorochrome used (e.g. CD4-FITC).
- The axis scales are clearly visible. Include numbers along axes only for bottom left plot of group (a 'group' is an analysis of identical markers).
- All plots are contour plots with outliers or pseudocolor plots.
- A numerical value for number of cells or percentage (with statistics) is provided.

### Methodology

#### Sample preparation

Describe the sample preparation, detailing the biological source of the cells and any tissue processing steps used.

#### Instrument

Identify the instrument used for data collection, specifying make and model number.

#### Software

Describe the software used to collect and analyze the flow cytometry data. For custom code that has been deposited into a community repository, provide accession details.

#### Cell population abundance

Describe the abundance of the relevant cell populations within post-sort fractions, providing details on the purity of the samples and how it was determined.

#### Gating strategy

Describe the gating strategy used for all relevant experiments, specifying the preliminary FSC/SSC gates of the starting cell population, indicating where boundaries between "positive" and "negative" staining cell populations are defined.

- Tick this box to confirm that a figure exemplifying the gating strategy is provided in the Supplementary Information.



## Experimental design

Design type	<i>Indicate task or resting state; event-related or block design.</i>
Design specifications	<i>Specify the number of blocks, trials or experimental units per session and/or subject, and specify the length of each trial or block (if trials are blocked) and interval between trials.</i>
Behavioral performance measures	<i>State number and/or type of variables recorded (e.g. correct button press, response time) and what statistics were used to establish that the subjects were performing the task as expected (e.g. mean, range, and/or standard deviation across subjects).</i>

## Acquisition

Imaging type(s)	<i>Specify: functional, structural, diffusion, perfusion.</i>
Field strength	<i>Specify in Tesla</i>
Sequence & imaging parameters	<i>Specify the pulse sequence type (gradient echo, spin echo, etc.), imaging type (EPI, spiral, etc.), field of view, matrix size, slice thickness, orientation and TE/TR/flip angle.</i>
Area of acquisition	<i>State whether a whole brain scan was used OR define the area of acquisition, describing how the region was determined.</i>
Diffusion MRI	<input type="checkbox"/> Used <input type="checkbox"/> Not used

## Preprocessing

Preprocessing software	<i>Provide detail on software version and revision number and on specific parameters (model/functions, brain extraction, segmentation, smoothing kernel size, etc.).</i>
Normalization	<i>If data were normalized/standardized, describe the approach(es): specify linear or non-linear and define image types used for transformation OR indicate that data were not normalized and explain rationale for lack of normalization.</i>
Normalization template	<i>Describe the template used for normalization/transformation, specifying subject space or group standardized space (e.g. original Talairach, MNI305, ICBM152) OR indicate that the data were not normalized.</i>
Noise and artifact removal	<i>Describe your procedure(s) for artifact and structured noise removal, specifying motion parameters, tissue signals and physiological signals (heart rate, respiration).</i>
Volume censoring	<i>Define your software and/or method and criteria for volume censoring, and state the extent of such censoring.</i>

## Statistical modeling & inference

Model type and settings	<i>Specify type (mass univariate, multivariate, RSA, predictive, etc.) and describe essential details of the model at the first and second levels (e.g. fixed, random or mixed effects; drift or auto-correlation).</i>
Effect(s) tested	<i>Define precise effect in terms of the task or stimulus conditions instead of psychological concepts and indicate whether ANOVA or factorial designs were used.</i>
Specify type of analysis:	<input type="checkbox"/> Whole brain <input type="checkbox"/> ROI-based <input type="checkbox"/> Both
Statistic type for inference	<i>Specify voxel-wise or cluster-wise and report all relevant parameters for cluster-wise methods.</i>
(See <a href="#">Eklund et al. 2016</a> )	
Correction	<i>Describe the type of correction and how it is obtained for multiple comparisons (e.g. FWE, FDR, permutation or Monte Carlo).</i>

## Models & analysis

n/a	Involved in the study
<input type="checkbox"/>	<input type="checkbox"/> Functional and/or effective connectivity
<input type="checkbox"/>	<input type="checkbox"/> Graph analysis
<input type="checkbox"/>	<input type="checkbox"/> Multivariate modeling or predictive analysis
Functional and/or effective connectivity	<i>Report the measures of dependence used and the model details (e.g. Pearson correlation, partial correlation, mutual information).</i>
Graph analysis	<i>Report the dependent variable and connectivity measure, specifying weighted graph or binarized graph,</i>

Graph analysis

*subject- or group-level, and the global and/or node summaries used (e.g. clustering coefficient, efficiency, etc.).*

Multivariate modeling and predictive analysis

*Specify independent variables, features extraction and dimension reduction, model, training and evaluation metrics.*